Supporting Information

Square Planar Gold(III) bis-(1,1'-dimethyl-3,3'-methylene-diimidazol-2,2'-diylidene) Trication as Efficient and Selective Receptor Towards Halogen Anions: Cooperative Effect of Au···X and X···HC Interactions

Marco Baron,[a] Anna Dall'Anese,[a] Cristina Tubaro,[a]* Laura Orian,[a] Valerio Di Marco,[a] Sara Bogialli,[a] Claudia Graiff,[b] Marino Basato[a]

[a] Dipartimento di Scienze Chimiche, Università degli Studi di Padova, via Marzolo 1, 35131 Padova, Italy.
E-mail: cristina.tubaro@unipd.it

[b] Dipartimento di Scienze Chimiche, della Vita e della Sostenibilità, Università degli Studi di Parma, Parco Area delle Scienze 17/A, 43124 Parma, Italy.

1. NMR spectra of compound 1-3Cl

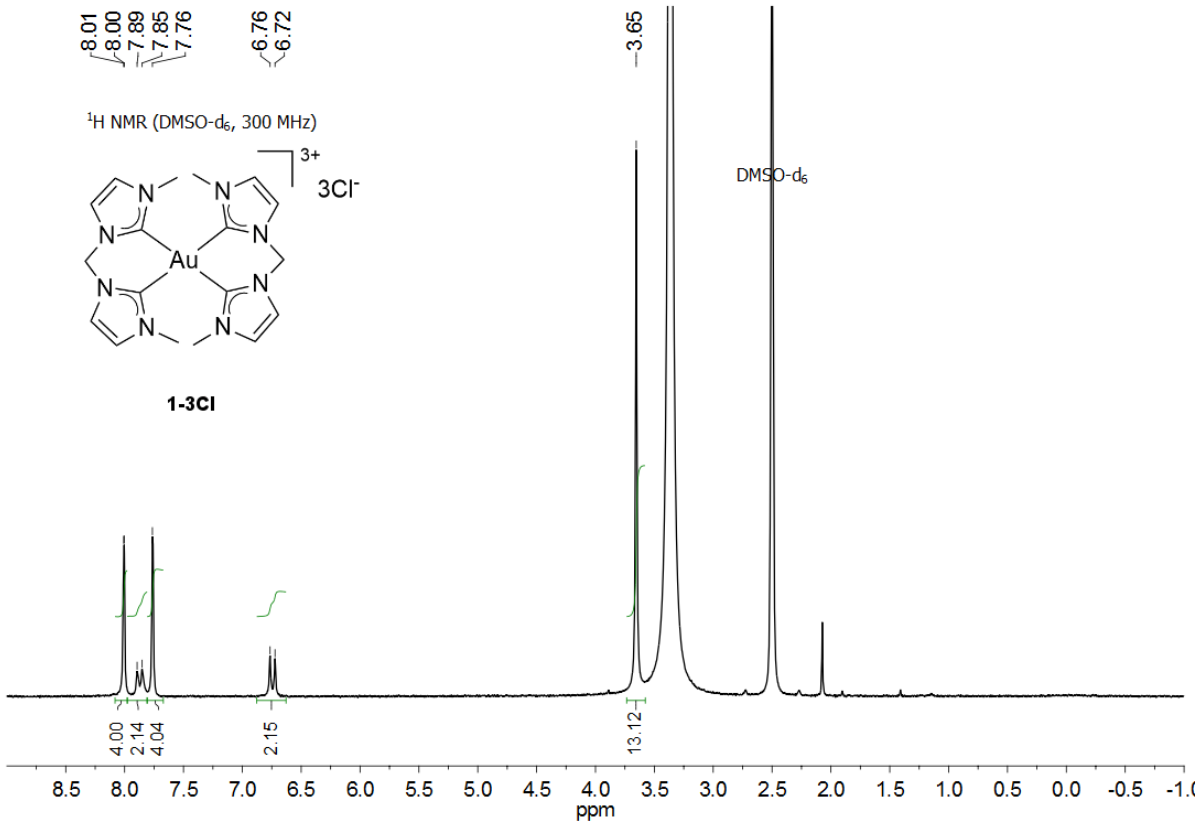

Figure S1: ^{1}H NMR (DMSO-d$_6$, 300 MHz) of **1-3Cl**.

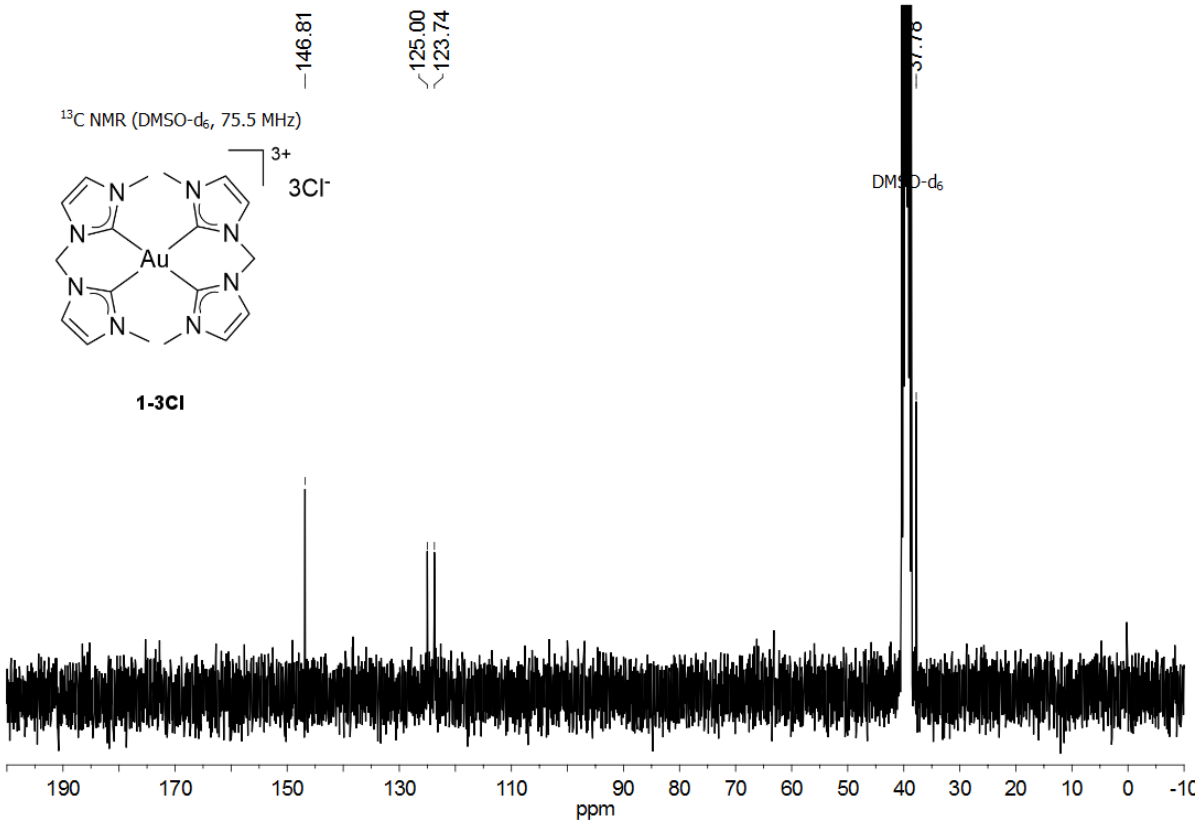

Figure S2: ^{13}C{^{1}H} NMR (DMSO-d$_6$, 75.5 MHz) of **1-3Cl**.

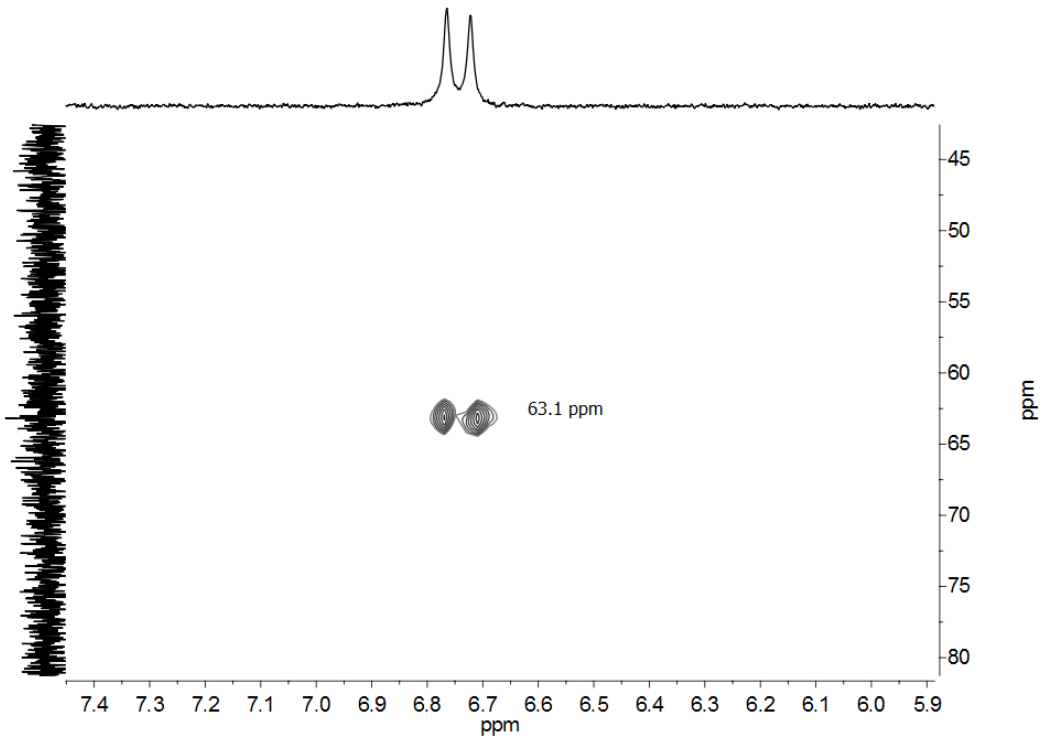

Figure S3: Section of the $^{1}H,^{13}C$ HMQC NMR (DMSO-d_6) of **1-3Cl**, showing the coupling between the methylene carbon and one of the two methylene protons.

2. NMR spectra of compound 1-3Br

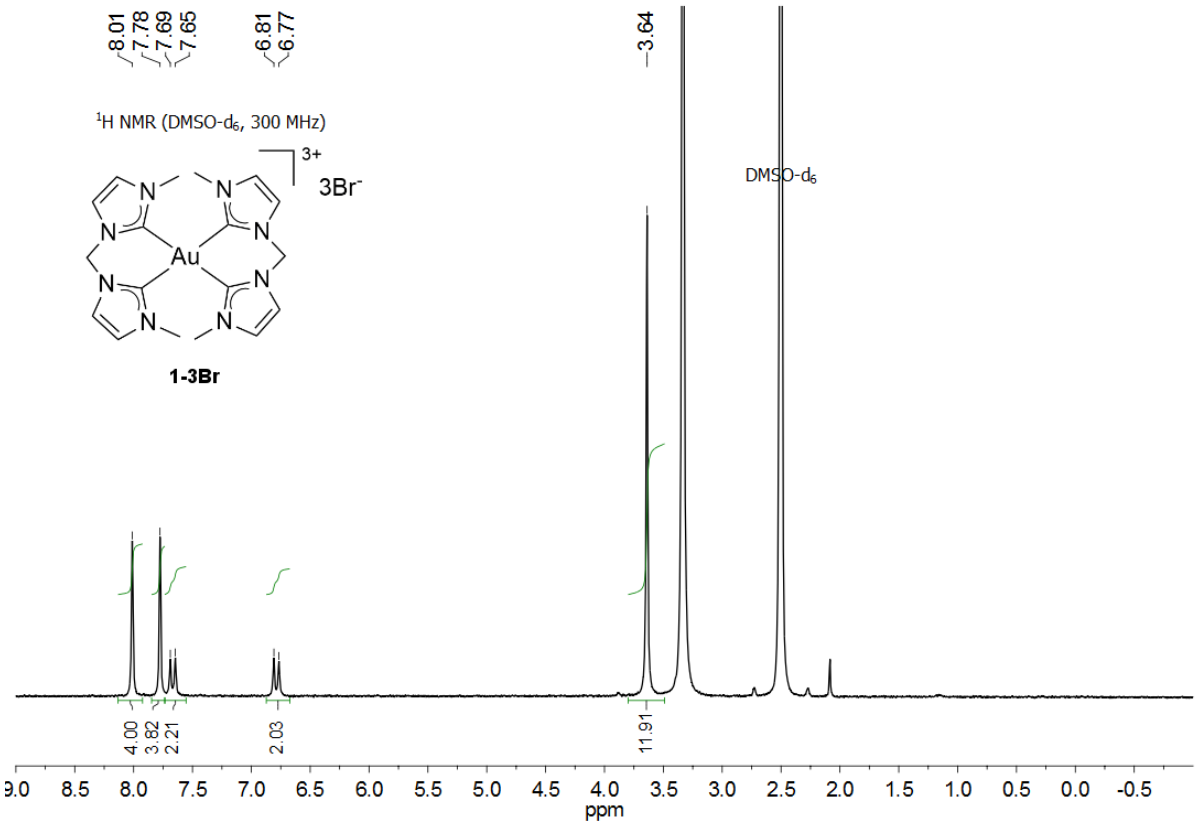

Figure S4: ^{1}H NMR (DMSO-d$_6$, 300 MHz) of **1-3Br**.

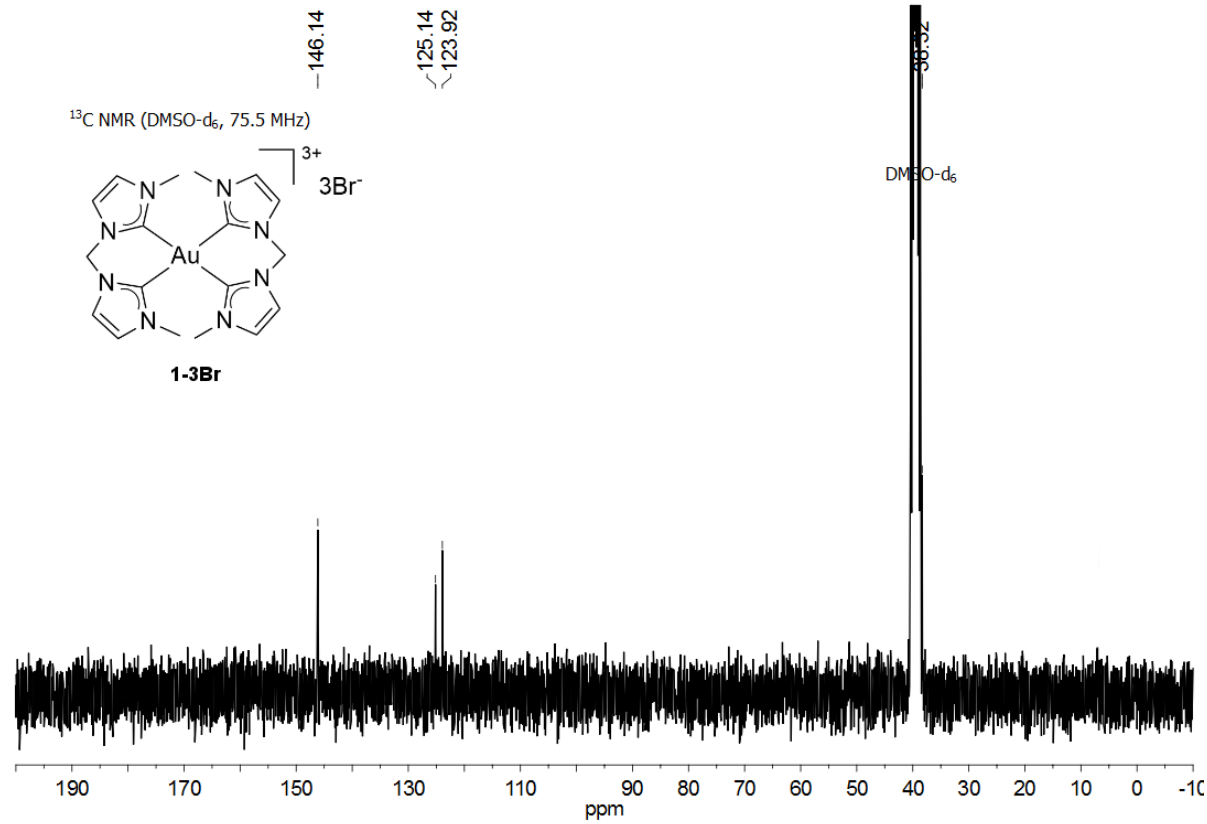

Figure S5: ^{13}C{^{1}H} NMR (DMSO-d$_6$, 75.5 MHz) of **1-3Br**.

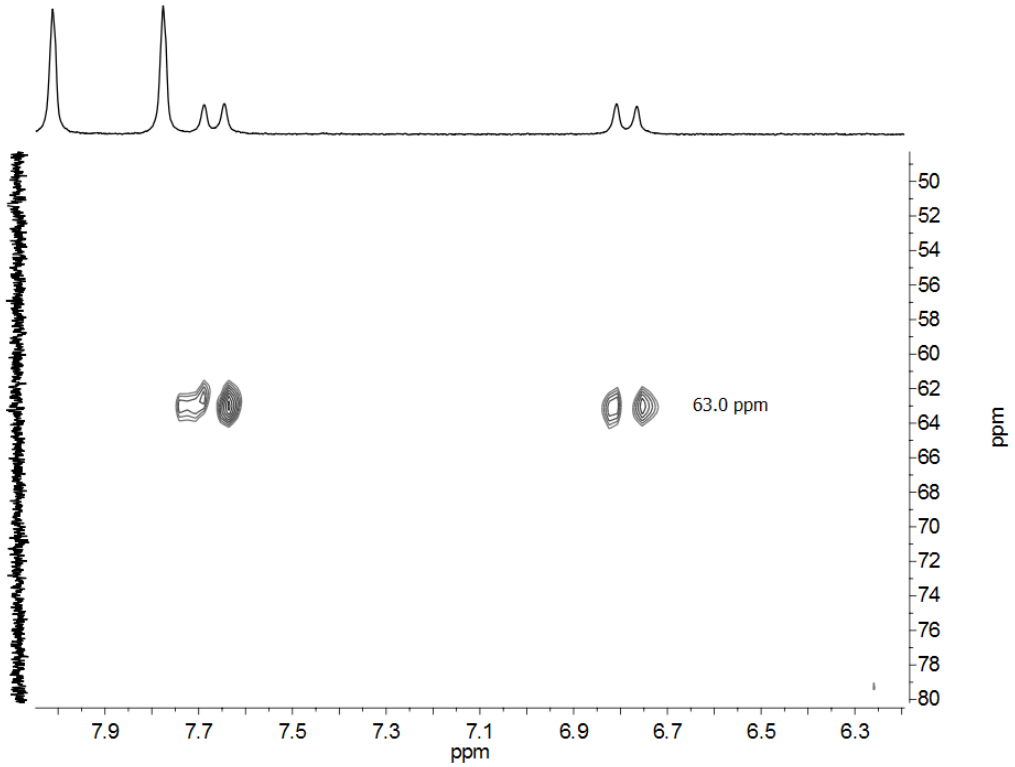

Figure S6: Section of the $^{1}H,^{13}C$ HMQC NMR (DMSO-d_6) of **1-3Br**, showing the coupling between the methylene carbon and the two methylene protons.

3. NMR spectra of compound 1-3I

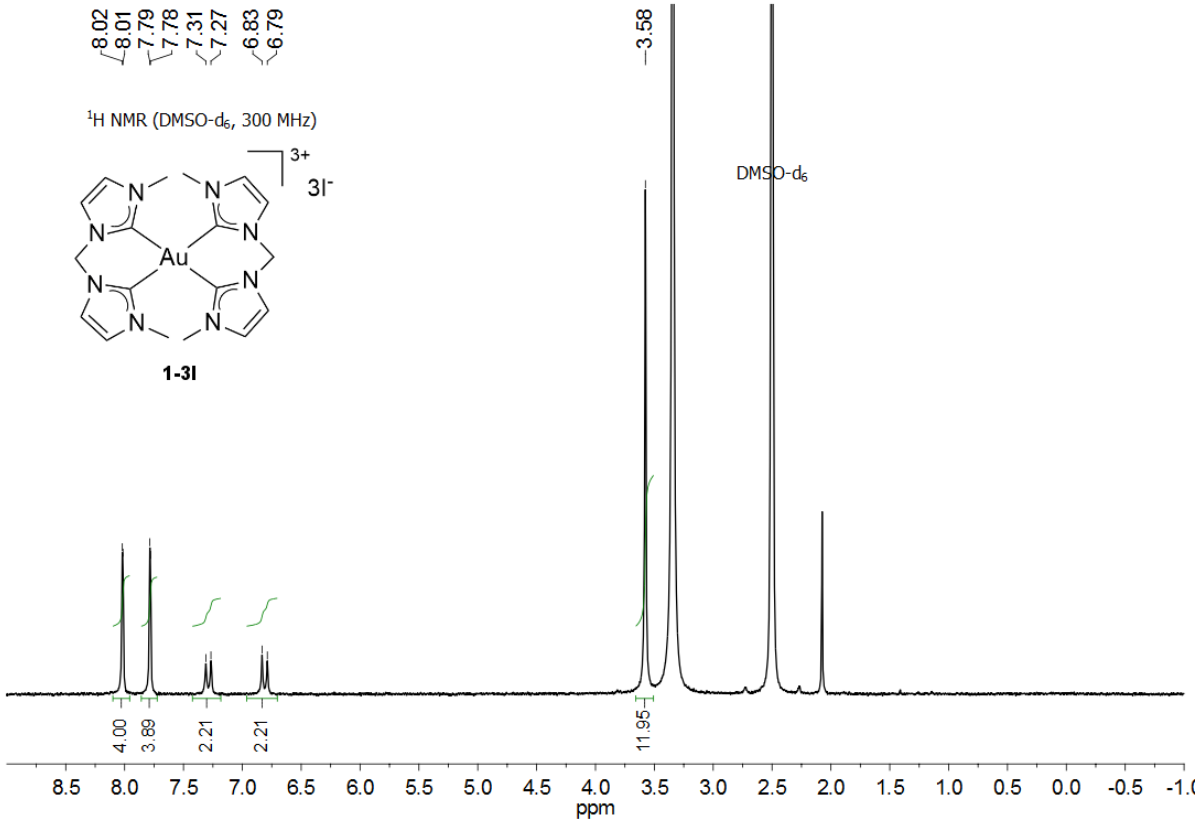

Figure S7: ^{1}H NMR (DMSO-d$_6$, 300 MHz) of **1-3I**.

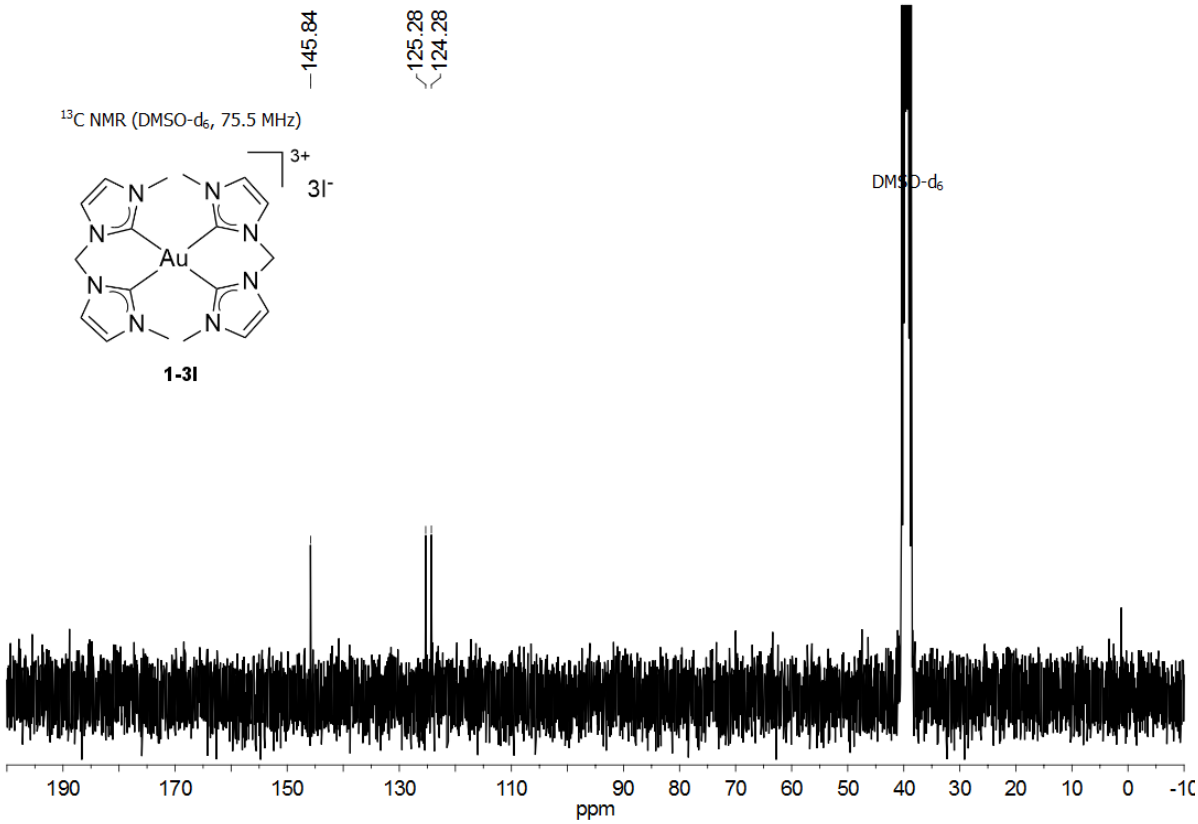

Figure S8: ^{13}C{^{1}H} NMR (DMSO-d$_6$, 75.5 MHz) of **1-3I**.

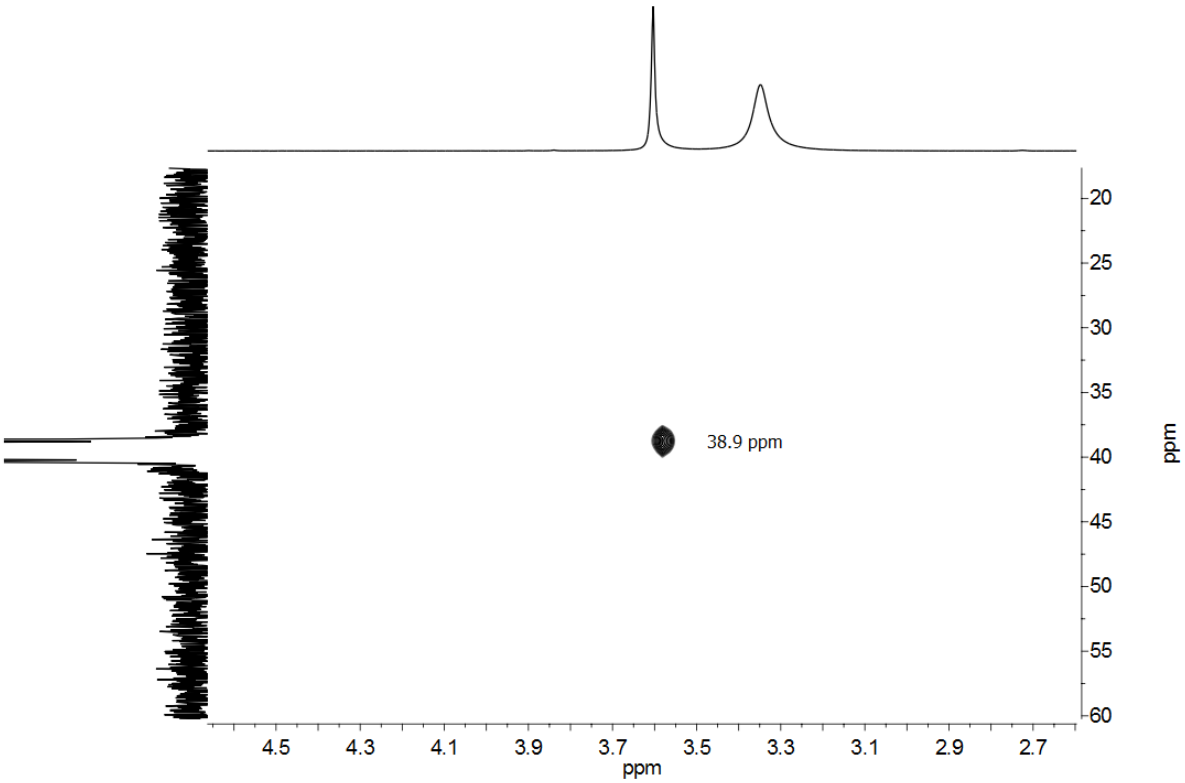

Figure S9: Section of the $^{1}H,^{13}C$ HMQC NMR (DMSO-d_6) of **1-3I**, showing the coupling between the methyl carbon and the methyl protons.

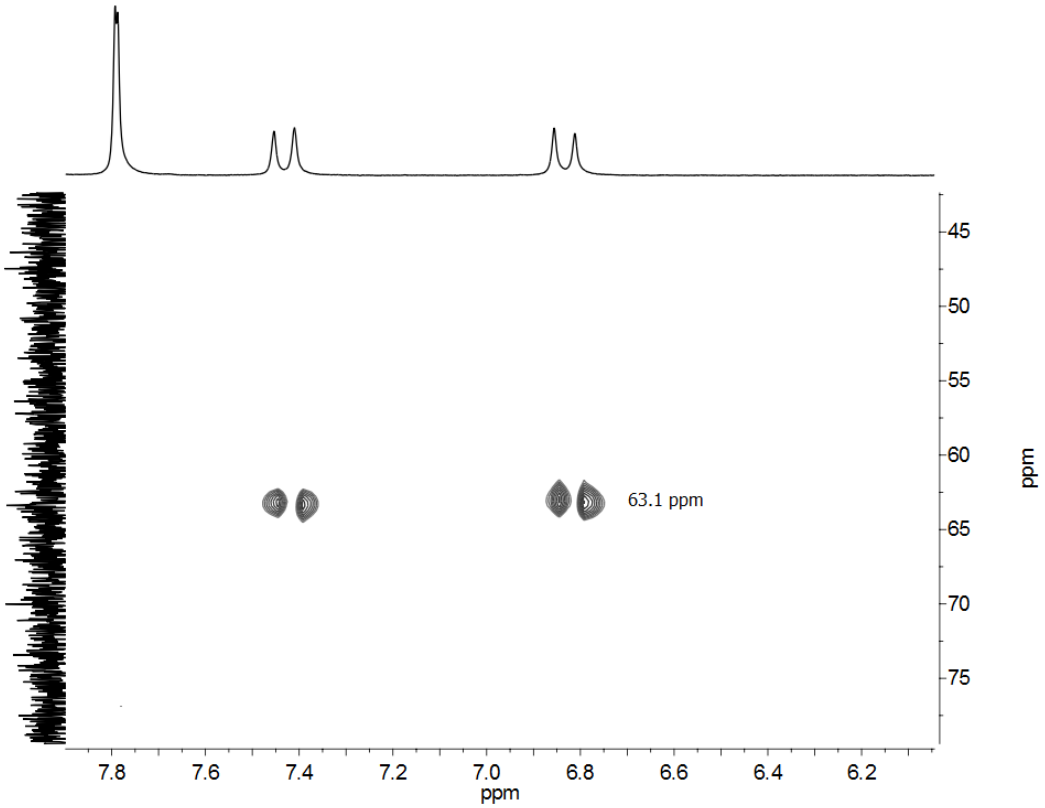

Figure S10: Section of the $^{1}H,^{13}C$ HMQC NMR (DMSO-d_6) of **1-3I**, showing the coupling between the methylene carbon and the two methylene protons.

4. HRMS spectra of complexes 1-3X

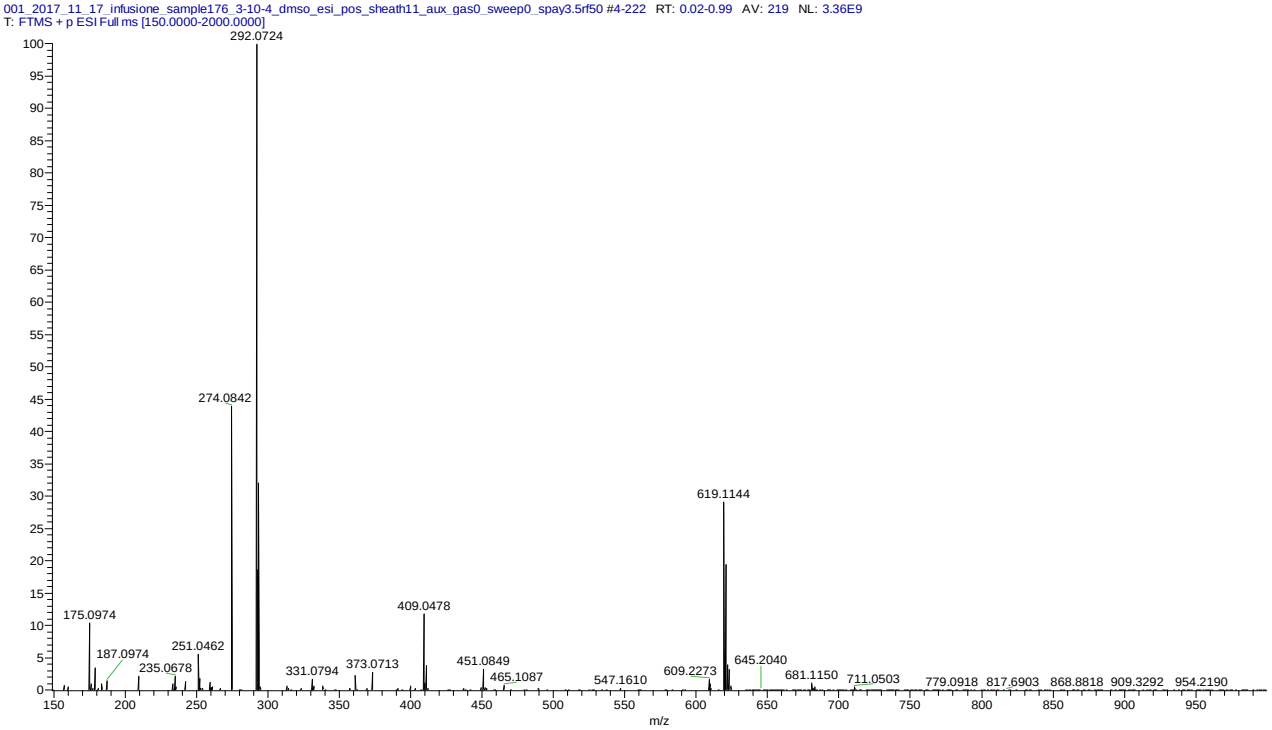

Figure S11: HRMS spectra of **1-3Cl** in DMSO ([**1-3Cl**]=0.33 mM).

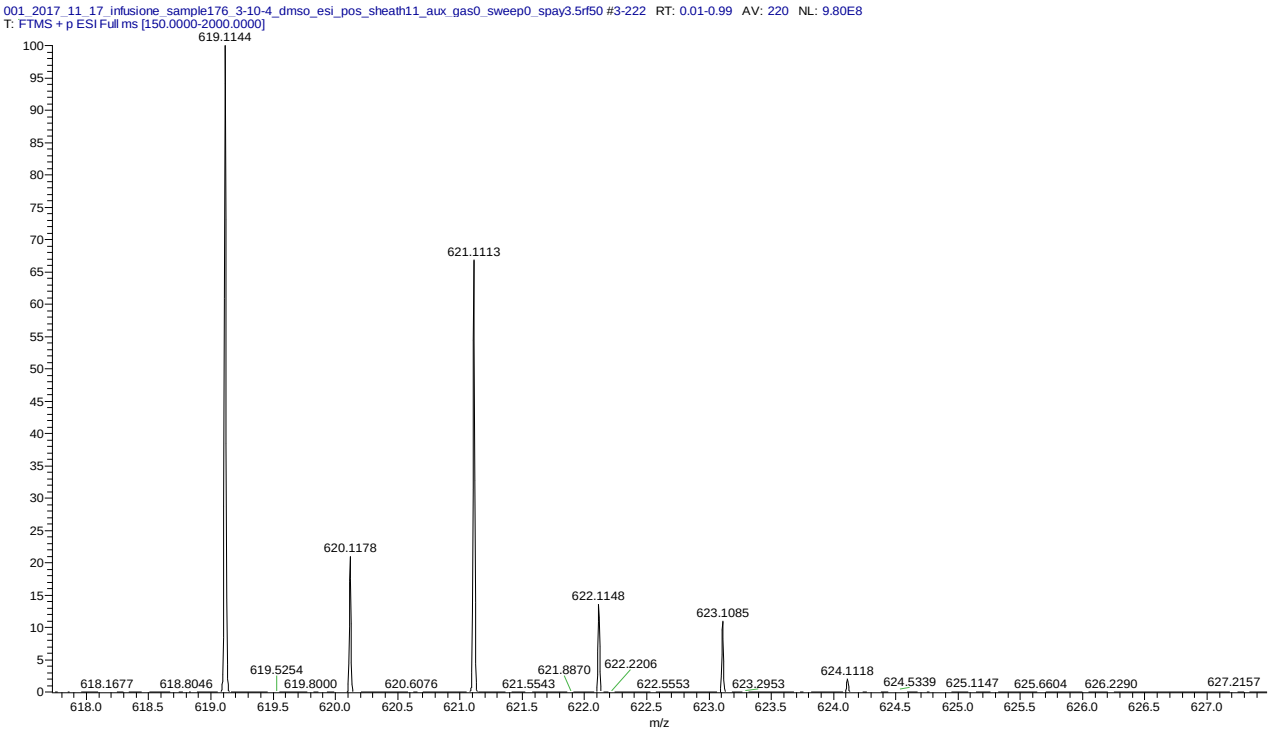

Figure S12: HRMS spectra of **1-3Cl** in DMSO ([**1-3Cl**]=0.33 mM): isotopic pattern of the peak at *m/z* 619.1144.

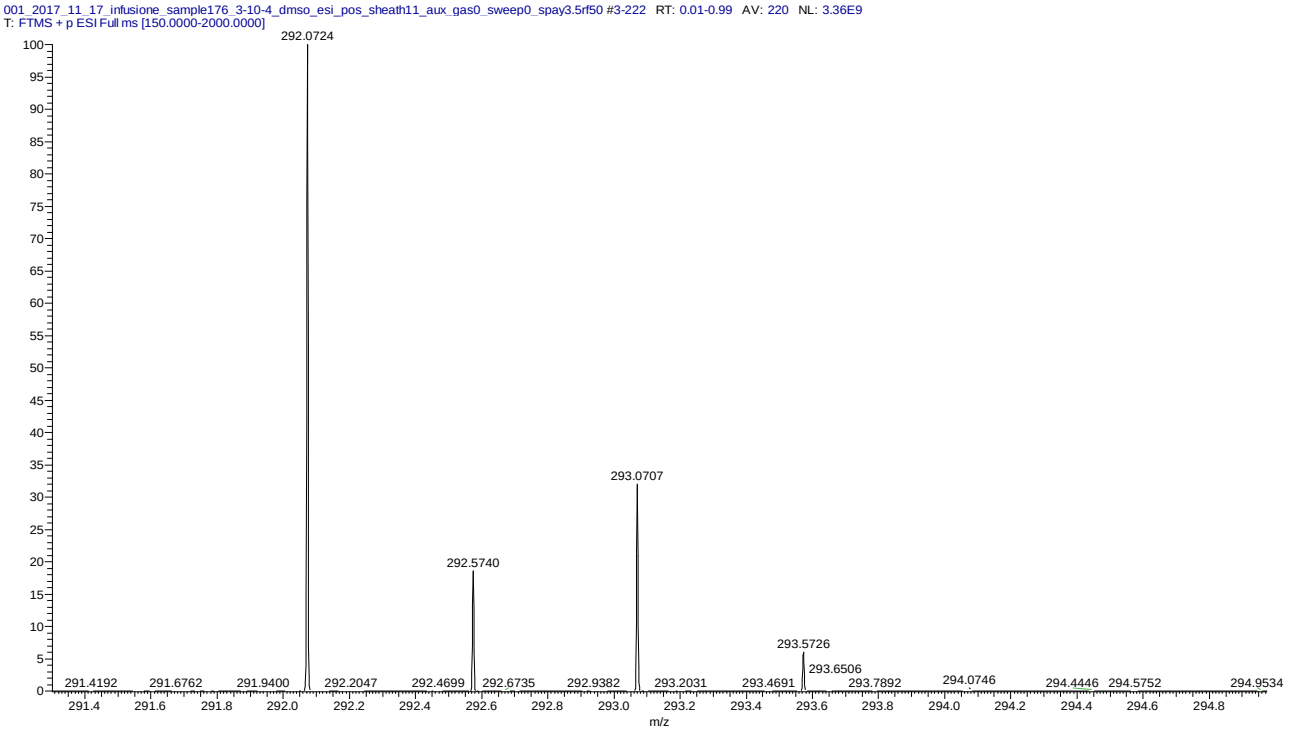

Figure S13: HRMS spectra of **1-3Cl** in DMSO ([**1-3Cl**]=0.33 mM): isotopic pattern of the peak at *m/z* 292.0724.

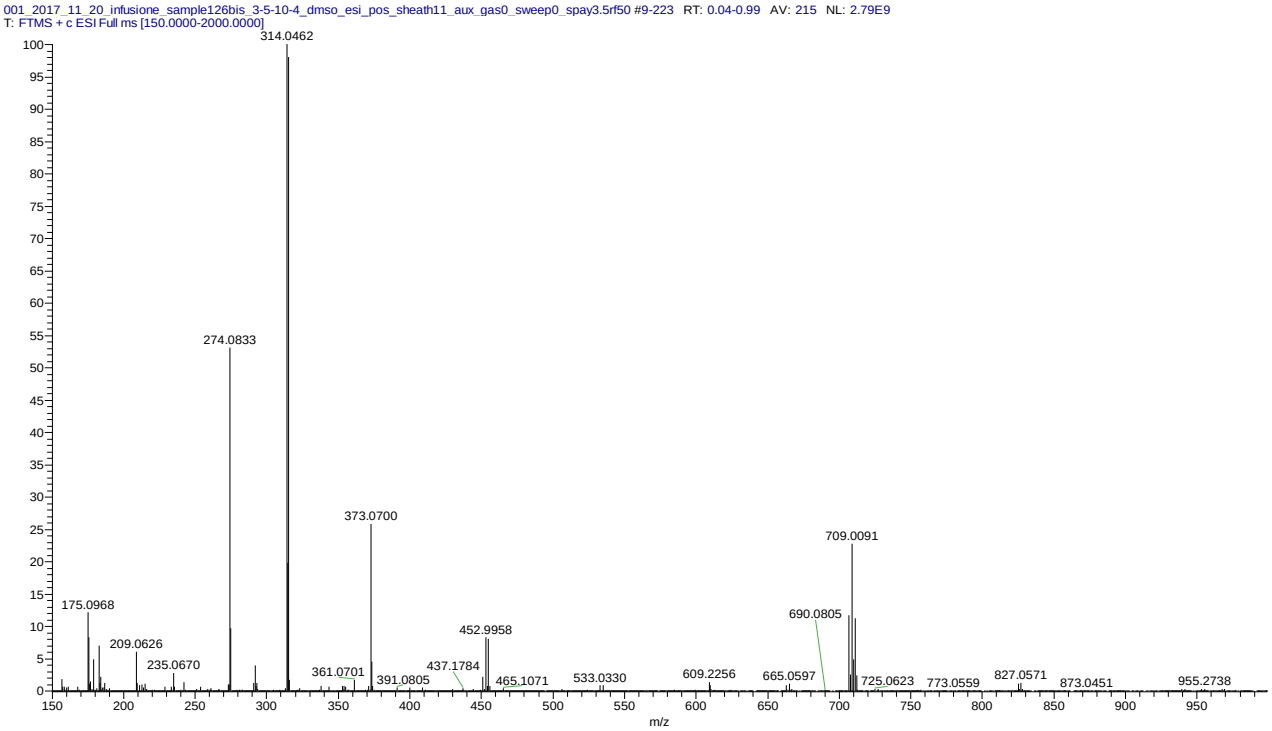

Figure S14: HRMS spectra of **1-3Br** in DMSO ([**1-3Br**]=0.35 mM).

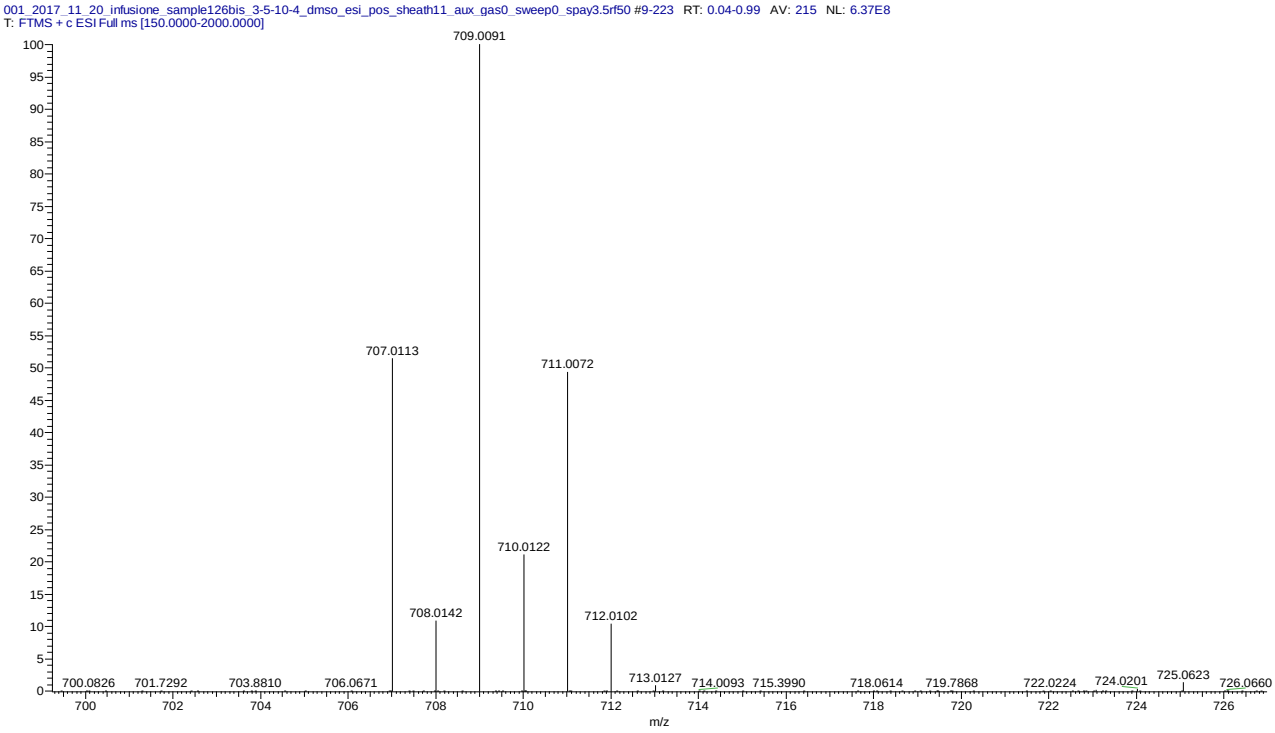

Figure S15: HRMS spectra of **1-3Br** in DMSO ([**1-3Br**]=0.35 mM): isotopic pattern of the peak at *m/z* 709.0091.

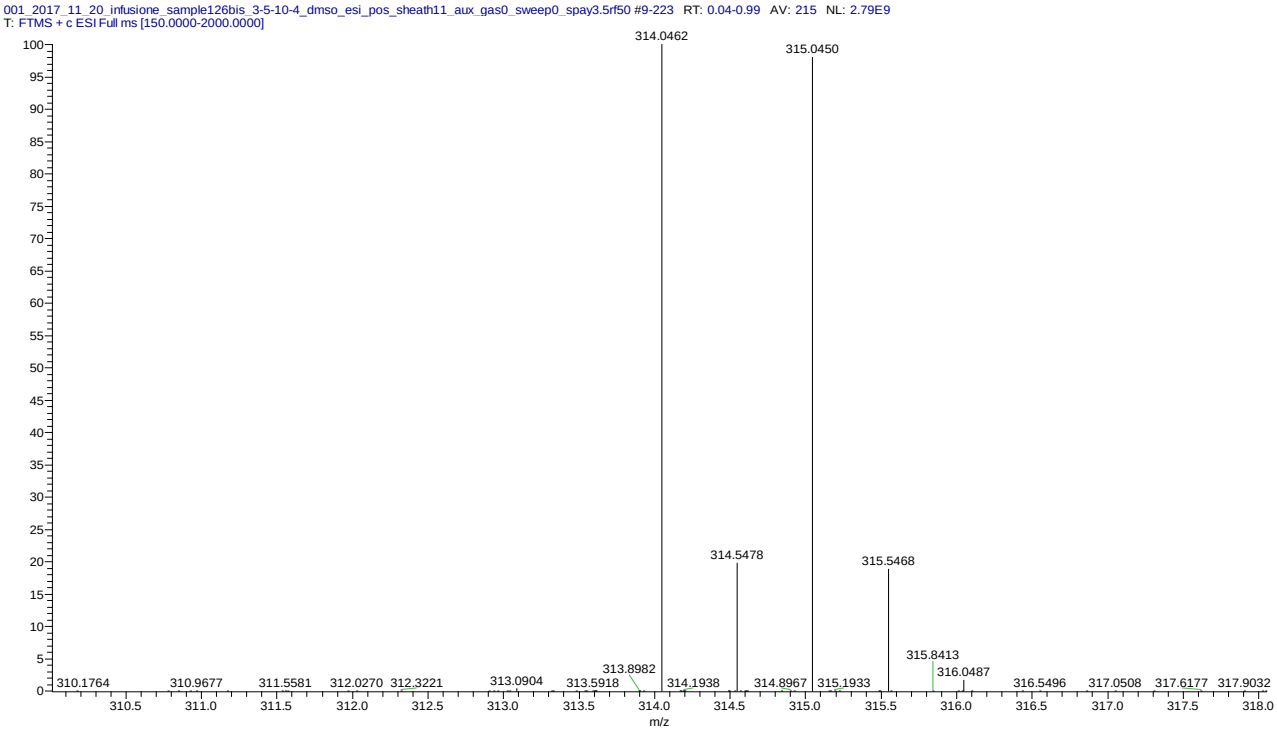

Figure S16: HRMS spectra of **1-3Br** in DMSO ([**1-3Br**]=0.35 mM): isotopic pattern of the peak at *m/z* 314.0462.

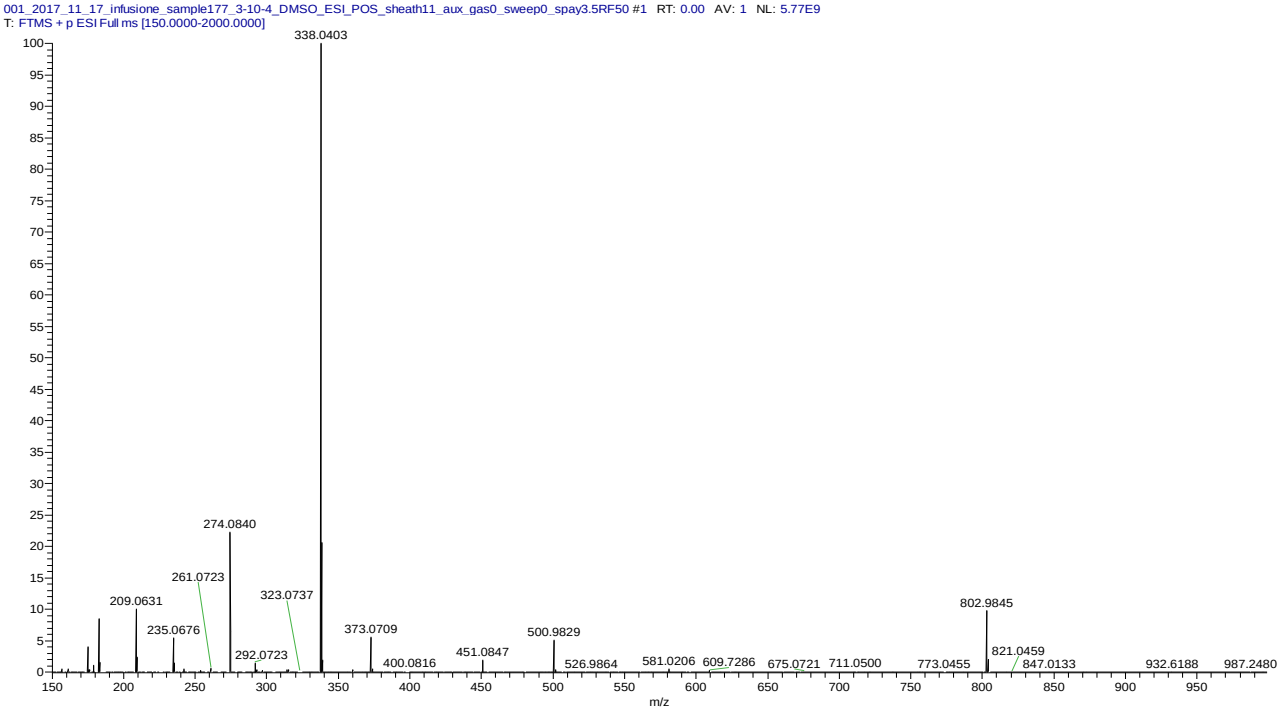

Figure S17: HRMS spectra of **1-3I** in DMSO ([**1-3I**]=0.34 mM).

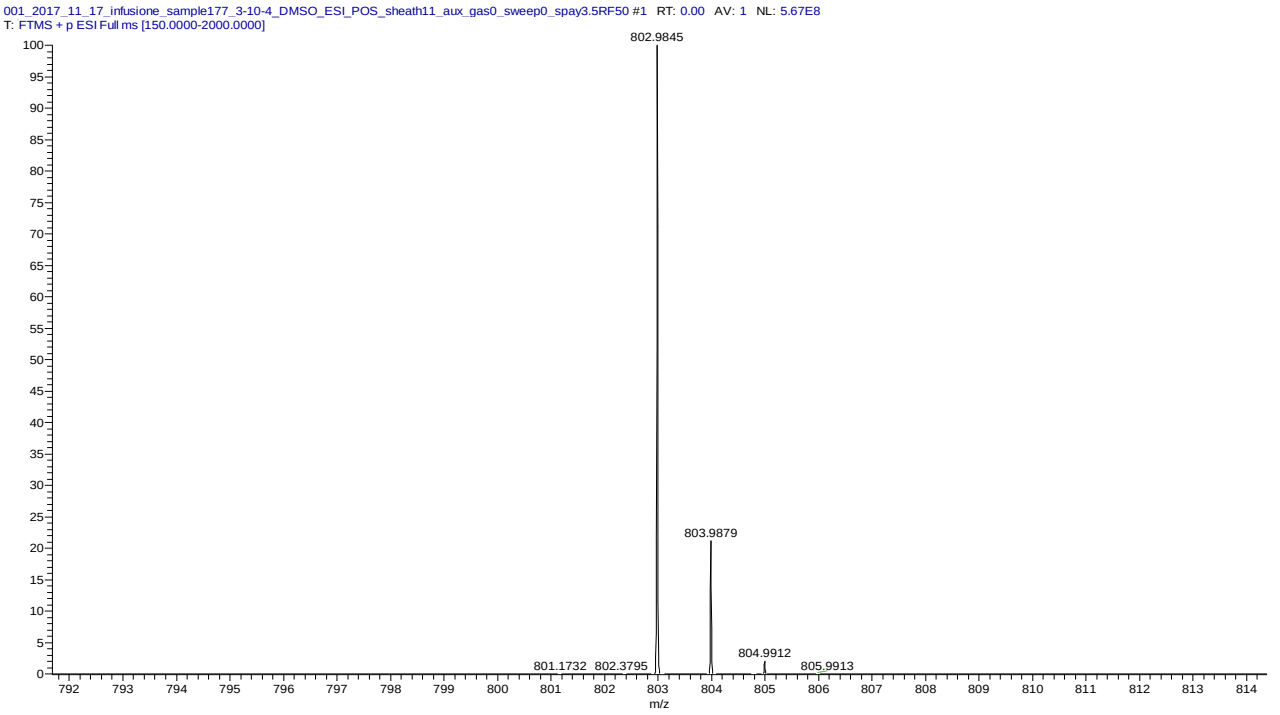

Figure S18: HRMS spectra of **1-3I** in DMSO ([**1-3I**]=0.34 mM): isotopic pattern of the peak at *m/z* 802.9845.

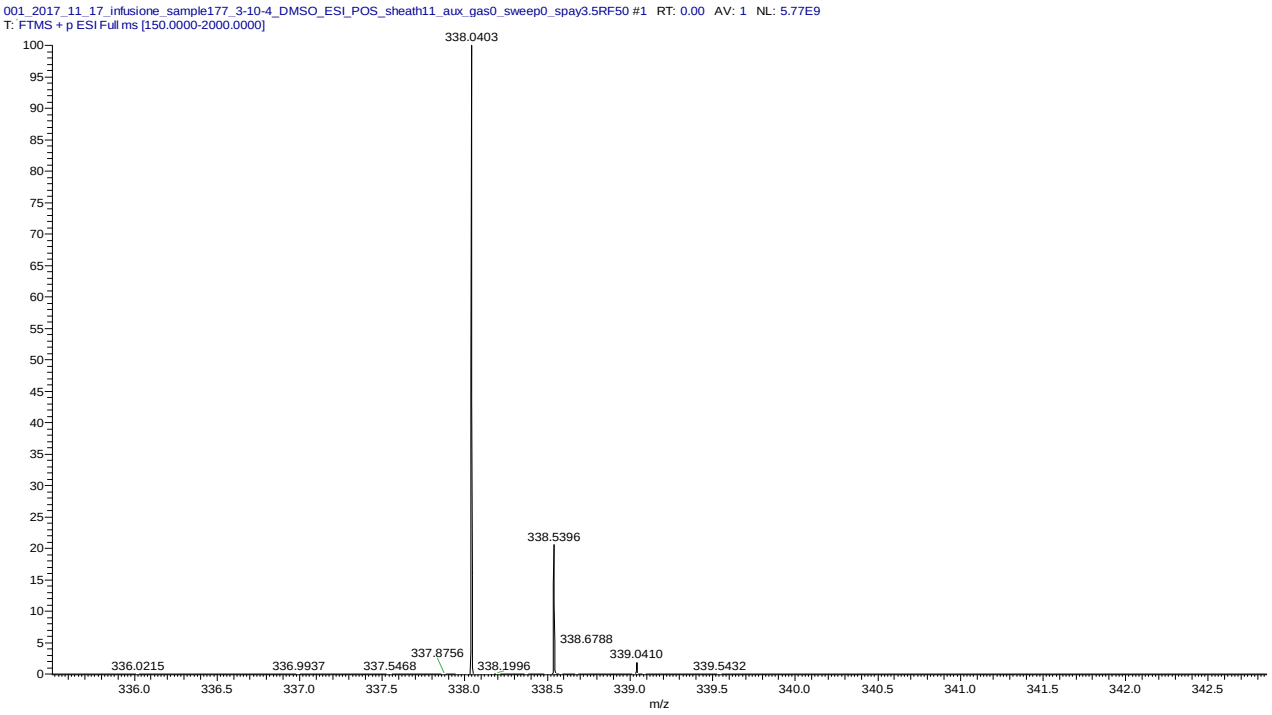

Figure S19: HRMS spectra of **1-3I** in DMSO ([**1-3I**]=0.34 mM): isotopic pattern of the peak at *m/z* 338.0403.

5. NMR titration of 1-3PF_6 with $NEt_4Cl{\cdot}H_2O$ to in dmso-d_6

Method a

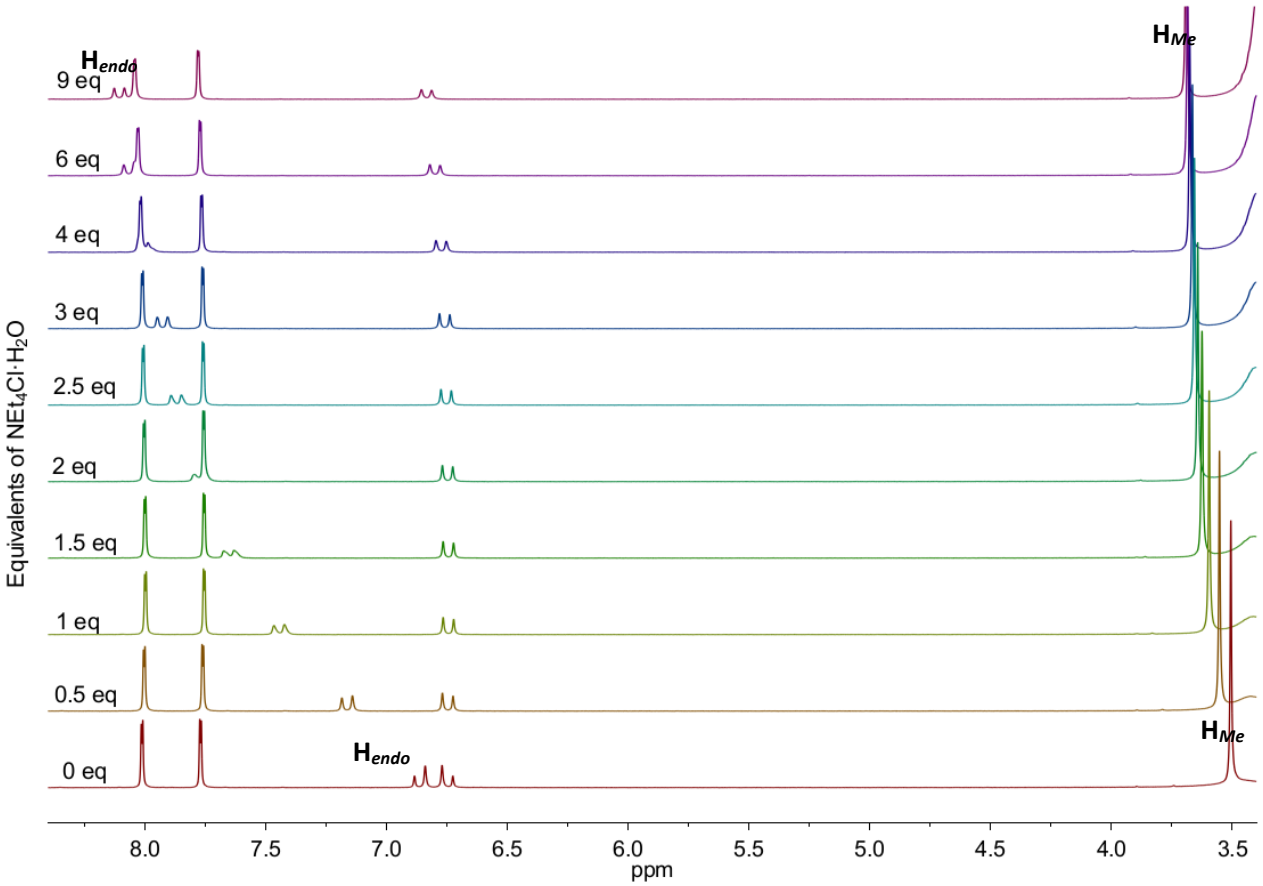

Figure S20: ^{1}H NMR titration (300 MHz, 298 K) of a $7.26{\cdot}10^{-3}$ M solution of **1-3PF_6** in DMSO-d_6 with a $NEt_4Cl{\cdot}H_2O$ solution in DMSO-d_6.

Table S1: ^{1}H NMR titration (300 MHz, 298 K) of a $7.26{\cdot}10^{-3}$ M solution of **1-3PF_6** in DMSO-d_6 with a $NEt_4Cl{\cdot}H_2O$ solution in DMSO-d_6.

[1-3PF_6] $(mM)_0$	$[Cl]_0/[1\text{-}3PF_6]_0$	δ H_{endo} (ppm)	Δδ H_{endo} (ppm)	δ H_{Me} (ppm)	Δδ H_{Me} (ppm)	$[Cl]_0$ (mM)
7.26	0	6.8625	0	3.506	0	0.00
7.21	0.5	7.16	0.2975	3.553	0.047	3.60
7.15	1	7.445	0.5825	3.595	0.089	7.15
7.10	1.5	7.65	0.7875	3.625	0.119	10.7
7.06	2	7.78	0.9175	3.643	0.137	14.1
7.01	2.5	7.87	1.0075	3.656	0.15	17.5
6.96	3	7.93	1.0675	3.665	0.159	20.9
6.86	4	8	1.1375	3.676	0.17	27.5
6.68	6	8.065	1.2025	3.685	0.179	40.1
6.43	9	8.105	1.2425	3.691	0.185	57.9

5.1 Example of fitting of the experimental data

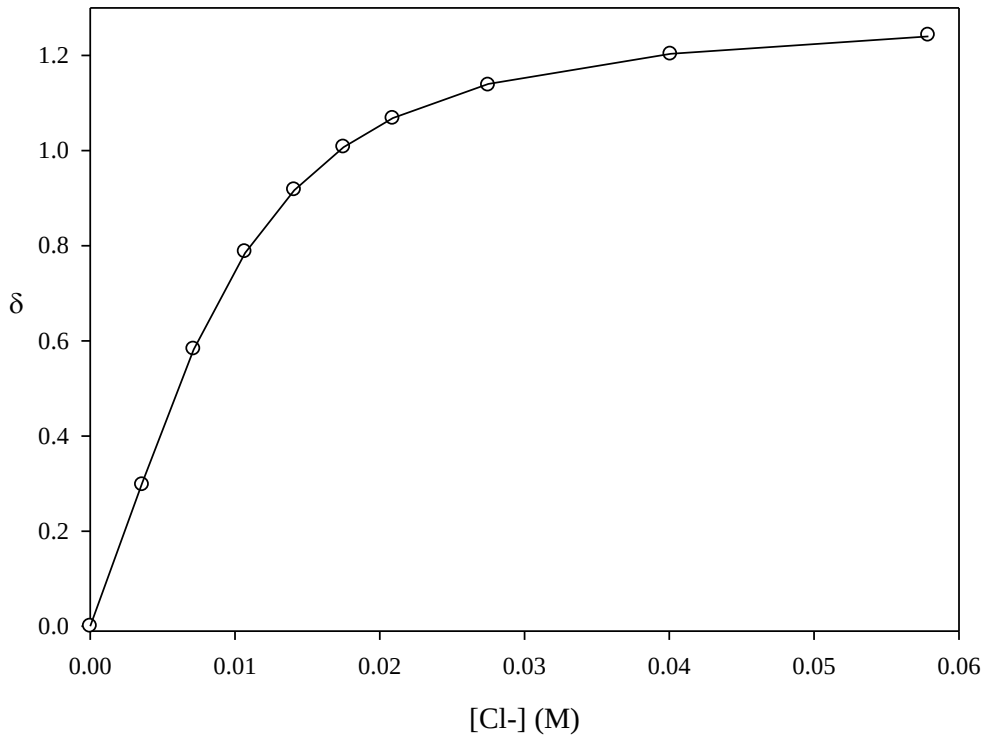

Figure S21: ^{1}H NMR experimental points (circles) obtained from the titration (300 MHz, 298 K) of a $7.26 \cdot 10^{-3}$ M solution of **1-3PF$_6$** in DMSO-d$_6$ with a $NEt_4Cl \cdot H_2O$ solution in DMSO-d$_6$. The lines represents the fitting of the experimental data.

The equation used for fitting is:

$$\delta = \frac{\Delta\delta_{CH_2\left(\mathbf{1}Cl^{2+}\right)}\left[\mathbf{1}Cl^{2+}\right] + \Delta\delta_{CH_2\left(\mathbf{1}Cl_2^{+}\right)}\left[\mathbf{1}Cl_2^{+}\right]}{C_{\mathbf{1}}}$$

where $\Delta\delta_{CH_2\left(\mathbf{1}Cl^{2+}\right)}$ and $\Delta\delta_{CH_2\left(\mathbf{1}Cl_2^{+}\right)}$ are the chemical shift values reported in Table 1 of the main text, [**1**Cl^{2+}] and [**1**Cl_2^{+}] are the concentrations of the complexes at equilibrium, computed by the fitting program using the equilibrium constants of Table 1, and $C_{\mathbf{1}}$ is the total concentration of **1**, reported in Table S1. Fitting parameters: mean sum of squares between experimental and computed values = 0.0017, mean variance = 0.00096.

Method b

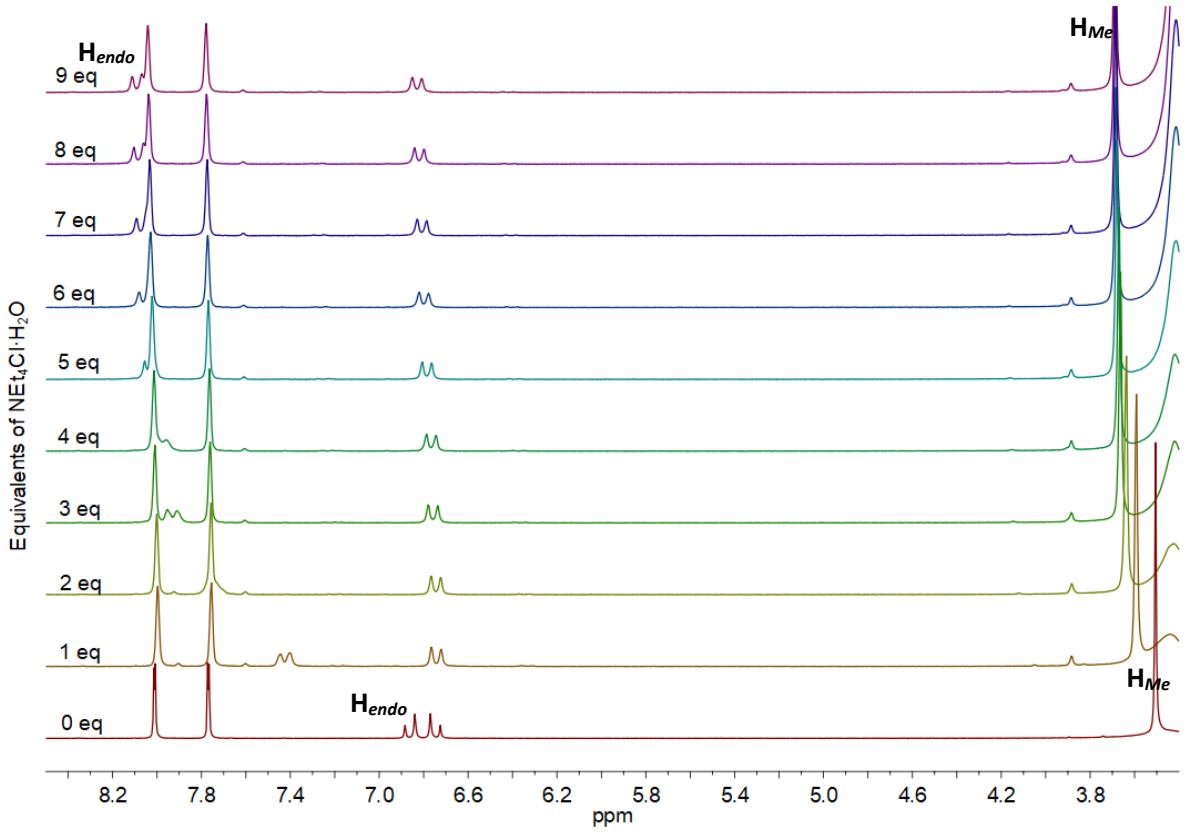

Figure S22: ^{1}H NMR titration (300 MHz, 298 K) of a $7.26 \cdot 10^{-3}$ M solution of **1-3PF$_6$** in DMSO-d$_6$ with a $NEt_4Cl \cdot H_2O$ solution in DMSO-d$_6$.

Table S2: ^{1}H NMR titration (300 MHz, 298 K) of a $7.26 \cdot 10^{-3}$ M solution of **1-3PF$_6$** in DMSO-d$_6$ with a $NEt_4Cl \cdot H_2O$ solution in DMSO-d$_6$.

[1-3PF$_6$] (mM)$_0$	[Cl]$_0$/[1-3PF$_6$]$_0$	δ H$_{endo}$ (ppm)	Δδ H$_{endo}$ (ppm)	δ H$_{Me}$ (ppm)	Δδ H$_{Me}$ (ppm)	[Cl]$_0$ (mM)
7.26	0	6.8625	0.00	3.506	0	0.00
7.26	1	7.42	0.5575	3.592	0.086	7.26
7.26	2	7.76	0.8975	3.637	0.131	14.52
7.26	3	7.93	1.0675	3.663	0.157	21.78
7.26	4	7.98	1.1175	3.669	0.163	29.04
7.26	5	8.04	1.1775	3.679	0.173	36.30
7.26	6	8.06	1.1975	3.683	0.177	43.56
7.26	7	8.07	1.2075	3.685	0.179	50.82
7.26	8	8.08	1.2175	3.687	0.181	58.08
7.26	9	8.09	1.2275	3.688	0.182	65.34

6. NMR titration of 1-3PF$_6$ with NEt$_4$Br in dmso-d_6

Method a

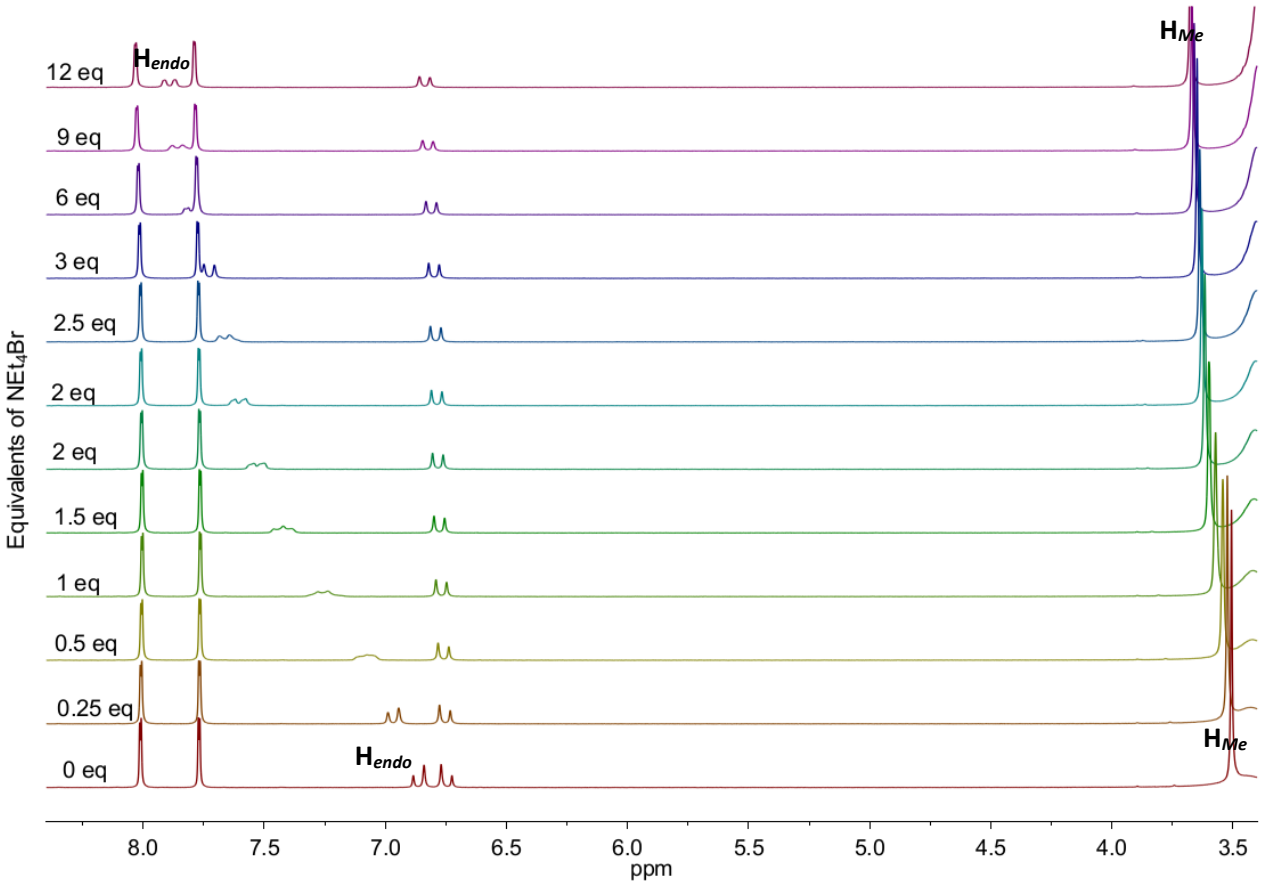

Figure S23: ^{1}H NMR titration (300 MHz, 298 K) of a 7.26·10^{-3} M solution of **1-3PF$_6$** in DMSO-d$_6$ with a NEt$_4$Br solution in DMSO-d$_6$.

Table S3: ^{1}H NMR titration (300 MHz, 298 K) of a 7.26·10^{-3} M solution of **1-3PF$_6$** in DMSO-d$_6$ with a NEt$_4$Br solution in DMSO-d$_6$.

[1-3PF$_6$]$_0$ (mM)	[Br]$_0$/[1-3PF$_6$]$_0$	δ H$_{endo}$ (ppm)	Δδ H$_{endo}$ (ppm)	δ H$_{Me}$ (ppm)	Δδ H$_{Me}$ (ppm)	[Br]$_0$ (mM)
7.26	0	6.8625	0	3.506	0	0.00
7.25	0.25	6.967	0.1045	3.523	0.017	1.81
7.21	0.5	7.077	0.2145	3.542	0.036	3.60
7.15	1	7.258	0.3955	3.571	0.065	7.15
7.10	1.5	7.421	0.5585	3.599	0.093	10.7
7.06	2	7.5265	0.664	3.616	0.11	14.1
7.01	2.5	7.6025	0.74	3.628	0.122	17.5
6.96	3	7.6635	0.801	3.637	0.131	20.9
6.86	4	7.7275	0.865	3.648	0.142	27.5
6.68	6	7.8045	0.942	3.66	0.154	40.1
6.43	9	7.859	0.9965	3.669	0.163	57.9
6.20	12	7.889	1.0265	3.675	0.169	74.3

7. NMR titration of 1-3PF_6 with NBu_4I in dmso-d_6

Method a

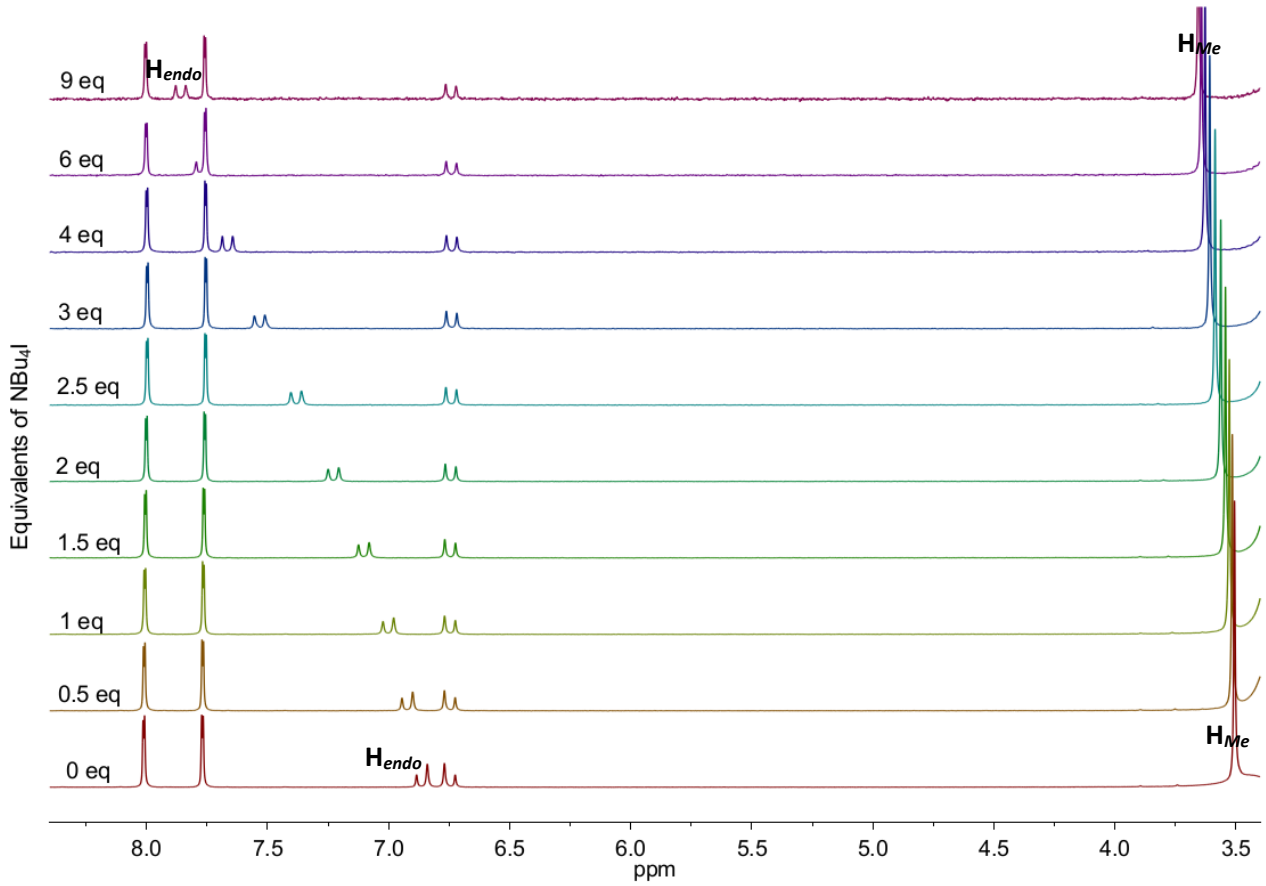

Figure S24: ^{1}H NMR titration (300 MHz, 298 K) of a $7.26 \cdot 10^{-3}$ M solution of **1-3PF_6** in DMSO-d_6 with a NBu_4I solution in DMSO-d_6.

Table S4: ^{1}H NMR titration (300 MHz, 298 K) of a $7.26 \cdot 10^{-3}$ M solution of **1-3PF_6** in DMSO-d_6 with a NBu_4I solution in DMSO-d_6.

$[1\text{-}3PF_6]_0$ (mM)	$[I]_0/[1\text{-}3PF_6]_0$	δH_{endo} (ppm)	$\Delta\delta H_{endo}$ (ppm)	δH_{Me} (ppm)	$\Delta\delta H_{Me}$ (ppm)	$[I]_0$ (mM)
7.26	0	6.863	0	3.506	0	0.00
7.21	0.5	7.036	0.173	3.535	0.029	3.60
7.15	1	7.1465	0.2835	3.553	0.047	7.15
7.10	1.5	7.214	0.351	3.565	0.059	10.7
7.06	2	7.271	0.408	3.575	0.069	14.1
7.01	2.5	7.321	0.458	3.583	0.077	17.5
6.96	3	7.353	0.49	3.589	0.083	20.9
6.86	4	7.4025	0.5395	3.599	0.093	27.5
6.68	6	7.462	0.599	3.61	0.104	40.1
6.43	9	7.513	0.65	3.619	0.113	57.9

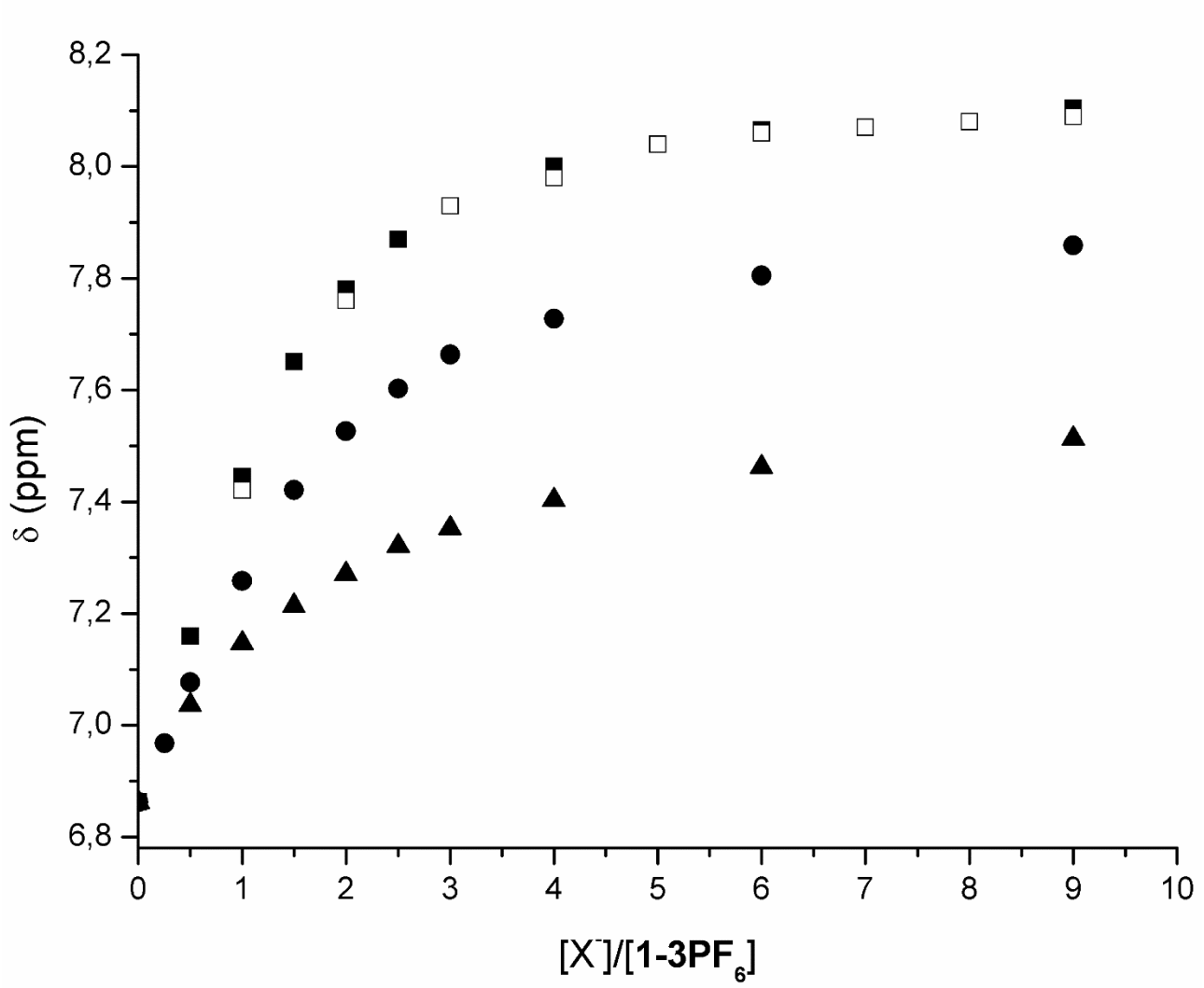

Figure S25: ^{1}H NMR titration curves (300 MHz, 298 K) based on the H_{endo} chemical shift variation of a $7.26 \cdot 10^{-3}$ M solution of **1-3PF$_6$** in DMSO-d_6 with a $NEt_4Cl \cdot H_2O$ (■, method a), $NEt_4Cl \cdot H_2O$ (□, method b), NEt_4Br (●) and NBu_4I (▲) solution in DMSO-d_6.

8. Job-Plot Titrations

8.1 ***1-3PF$_6$*** *and NEt$_4$Cl·H$_2$O in dmso-d$_6$*

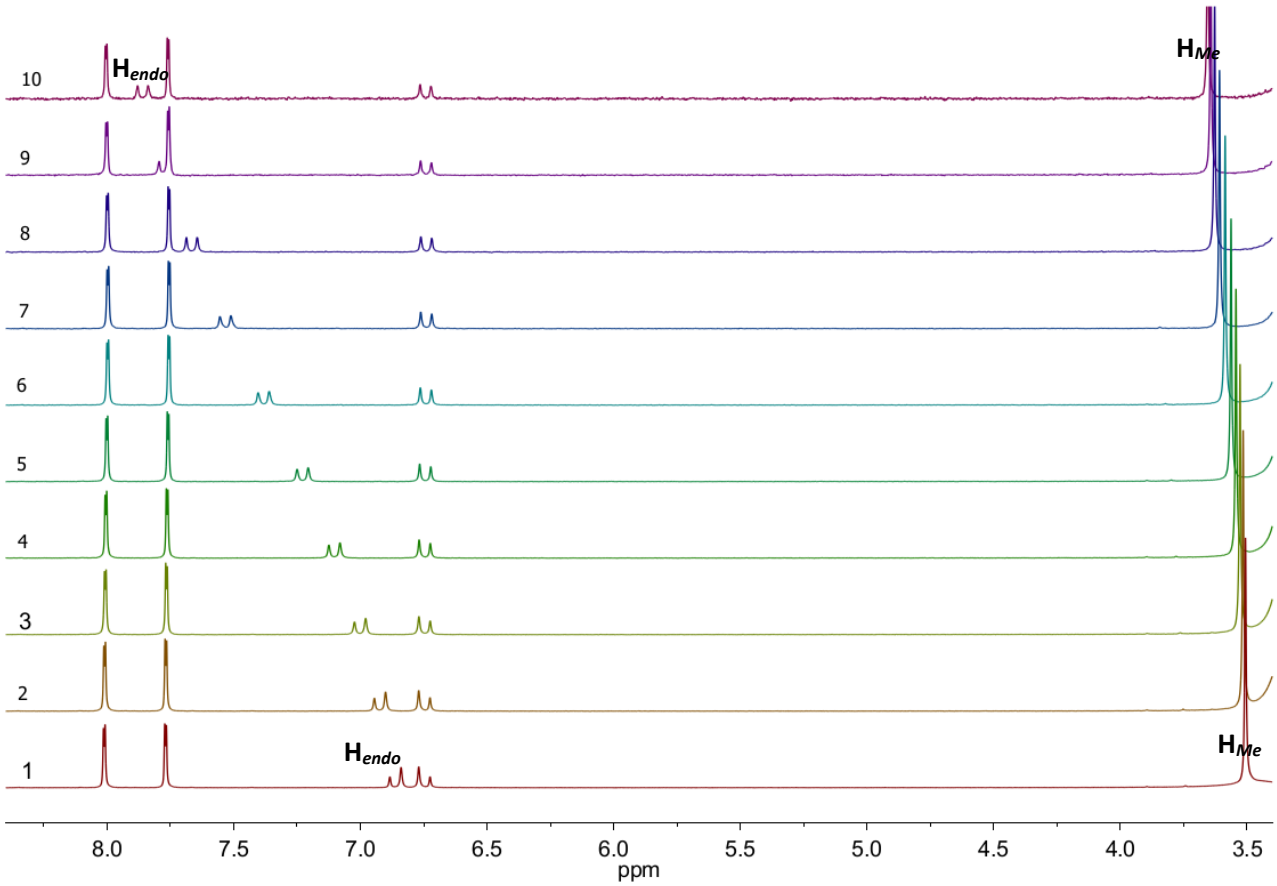

Figure S26: ^{1}H NMR spectra of Job plot titration in DMSO-d$_6$ for the interaction of **1-3PF$_6$** and Cl$^-$.

Table S5: ^{1}H NMR data of Job plot titration in DMSO-d$_6$ for the interaction of **1-3PF$_6$** and Cl$^-$.

n.	V (1-3PF$_6$)	V (Cl$^-$)	[1-3PF$_6$]$_0$	[Cl$^-$]$_0$	$\chi_{1\text{-}3PF6}$	Δ H$_{endo}$	Δδ H$_{endo}$	Δδ·$\chi_{1\text{-}3PF6}$ H$_{endo}$	δ H$_{Me}$	Δδ H$_{Me}$	Δδ·$\chi_{1\text{-}3PF6}$ H$_{Me}$
	(µL)	(µL)	(mM)	(mM)		(ppm)	(ppm)		(ppm)	(ppm)	
1	700	0	5.11	0.00	1	6.86	0	0	3.51	0	0
2	630	70	4.59	0.49	0.90	6.93	0.06	0.06	3.52	0.01	0.01
3	560	140	4.08	0.98	0.81	7.00	0.14	0.11	3.53	0.02	0.02
4	490	210	3.57	1.47	0.71	7.10	0.24	0.17	3.54	0.04	0.03
5	420	280	3.06	1.96	0.61	7.23	0.37	0.22	3.56	0.06	0.03
6	350	350	2.55	2.45	0.51	7.38	0.52	0.27	3.57	0.08	0.04
7	280	420	2.04	2.94	0.41	7.53	0.67	0.27	3.61	0.10	0.04
8	210	490	1.53	3.43	0.31	7.67	0.80	0.25	3.63	0.12	0.04
9	140	560	1.02	3.92	0.21	7.78	0.92	0.19	3.64	0.14	0.03
10	70	630	0.51	4.41	0.10	7.86	0.97	0.10	3.66	0.15	0.02
11	0	700	0.00	4.90	0	-	-	0	-	-	0

8.2 ***1-3PF$_6$*** *and NEt$_4$Br dmso-d$_6$*

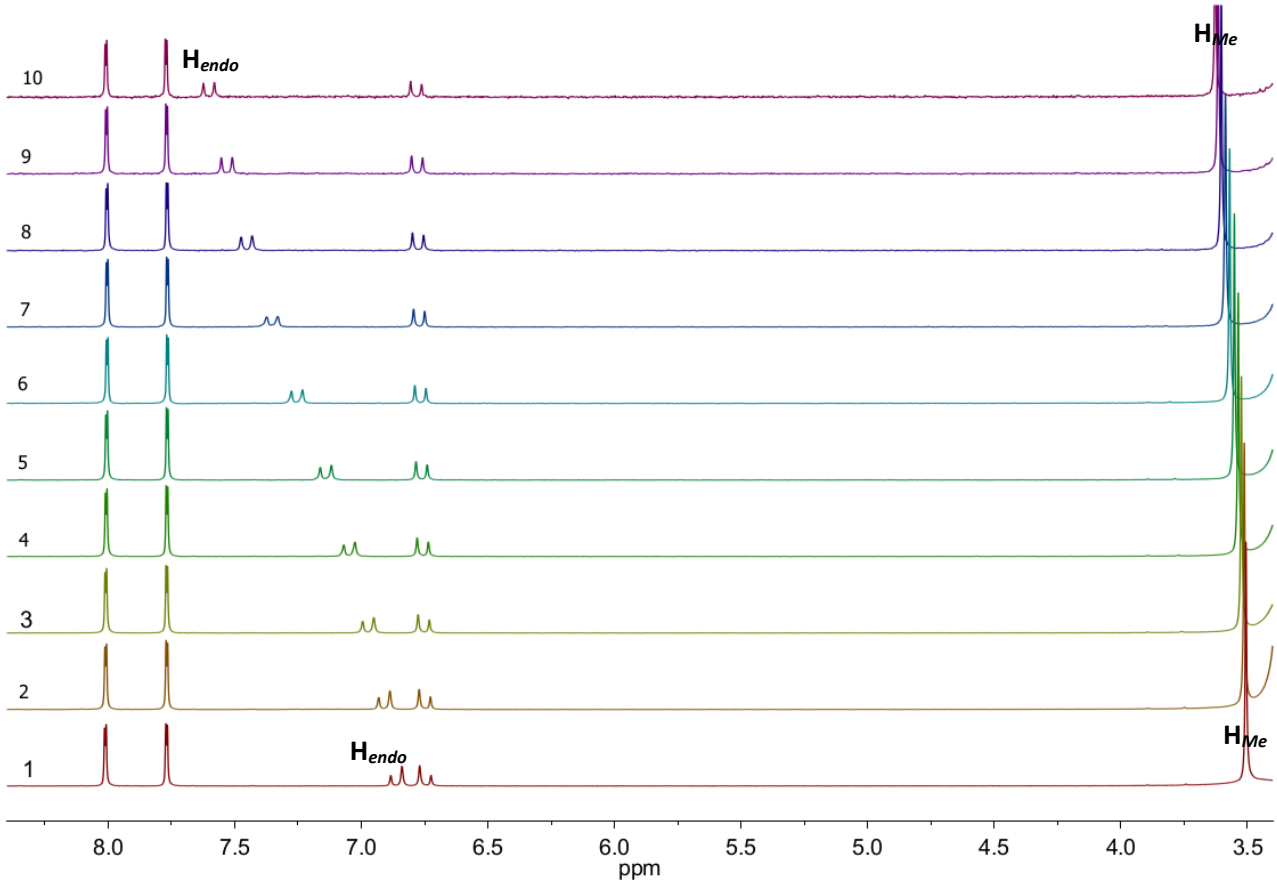

Figure S27: ^{1}H NMR spectra of Job plot titration in DMSO-d$_6$ for the interaction of **1-3PF$_6$** and Br$^-$.

Table S6: ^{1}H NMR data of Job plot titration in DMSO-d$_6$ for the interaction of **1-3PF$_6$** and Br$^-$.

n.	V (1-3PF$_6$)	V (Br$^-$)	[1-3PF$_6$]$_0$	[Br$^-$]$_0$	$\chi_{1\text{-}3PF6}$	Δ H$_{endo}$	Δδ H$_{endo}$	Δδ·$\chi_{1\text{-}3PF6}$ H$_{endo}$	δ H$_{Me}$	Δδ H$_{Me}$	Δδ·$\chi_{1\text{-}3PF6}$ H$_{Me}$
	(μL)	(μL)	(mM)	(mM)		(ppm)	(ppm)		(ppm)	(ppm)	
1	500	0	5.08	0	1.00	6.86	0.00	0.00	3.51	0.00	0.00
2	450	50	4.57	0.49	0.90	6.91	0.05	0.04	3.51	0.01	0.01
3	400	100	4.06	0.98	0.81	6.97	0.11	0.09	3.52	0.02	0.01
4	350	150	3.56	1.48	0.71	7.05	0.18	0.13	3.54	0.03	0.02
5	300	200	3.05	1.97	0.61	7.14	0.28	0.17	3.55	0.05	0.03
6	250	250	2.54	2.46	0.51	7.25	0.39	0.20	3.57	0.06	0.03
7	200	300	2.03	2.95	0.41	7.35	0.49	0.20	3.59	0.08	0.03
8	150	350	1.52	3.44	0.31	7.45	0.59	0.18	3.60	0.10	0.03
9	100	400	1.02	3.93	0.21	7.53	0.67	0.14	3.62	0.11	0.02
10	50	450	0.51	4.43	0.10	7.60	0.74	0.08	3.63	0.12	0.01
11	0	500	0	4.92	0.00	0.00	0.00	0.00	0.00	0.00	0.00

8.3 ***1-3PF$_6$*** *and NBu$_4$I dmso-d$_6$*

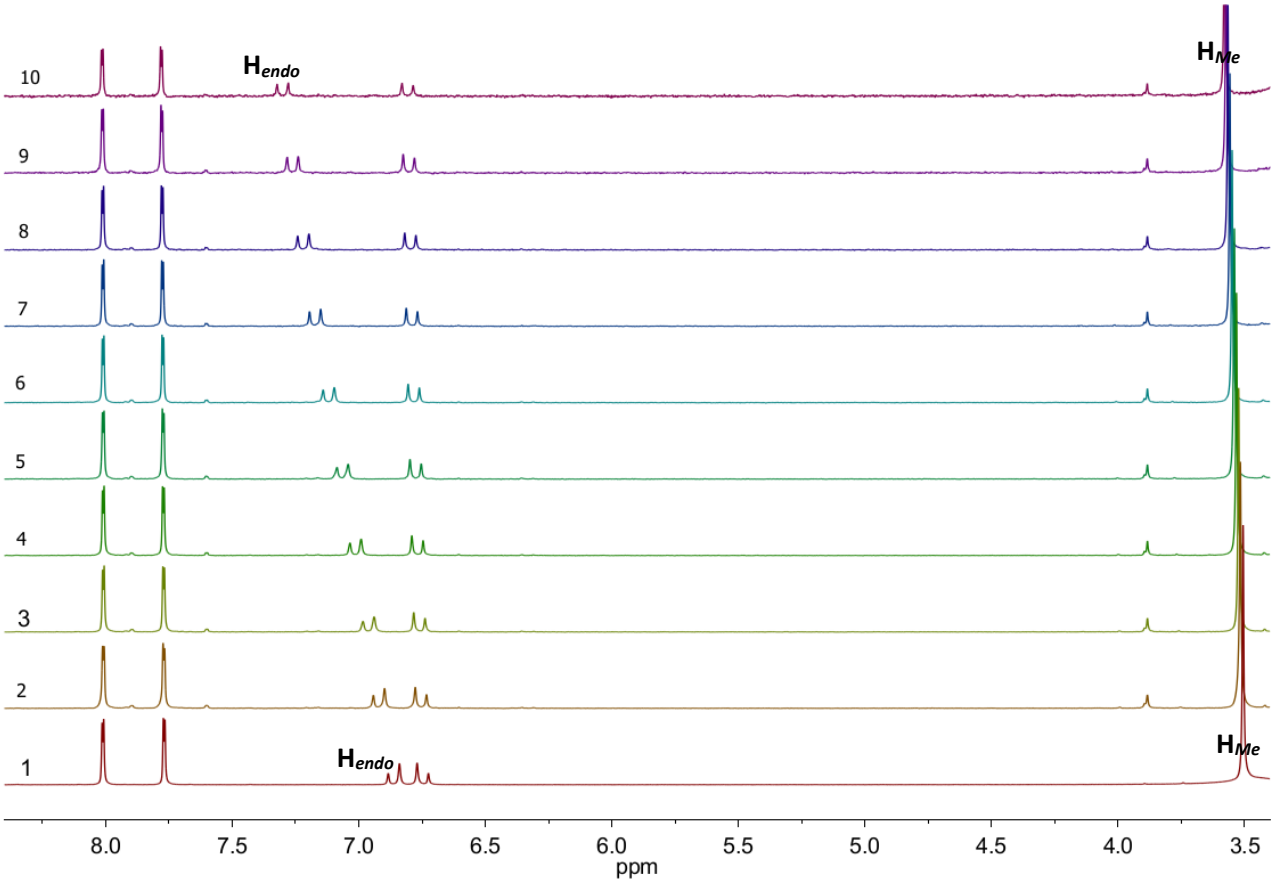

Figure S28: ^{1}H NMR spectra of Job plot titration in DMSO-d$_6$ for the interaction of **1-3PF$_6$** and I$^-$.

Table S7: ^{1}H NMR data of Job plot titration in DMSO-d$_6$ for the interaction of **1-3PF$_6$** and I$^-$.

n.	V (1-3PF$_6$)	V (I$^-$)	[1-3PF$_6$]$_0$	[I$^-$]$_0$	$\chi_{1\text{-}3PF6}$	Δ H_{endo}	Δδ H_{endo}	Δδ·$\chi_{1\text{-}3PF6}$ H_{endo}	δ H_{Me}	Δδ H_{Me}	Δδ·$\chi_{1\text{-}3PF6}$ H_{Me}
	(µL)	(µL)	(mM)	(mM)		(ppm)	(ppm)		(ppm)	(ppm)	
1	500	0	5.08	0.00	1.00	6.86	0.00	0.00	3.51	0.00	0.00
2	450	50	4.57	0.51	0.90	6.92	0.06	0.05	3.52	0.01	0.01
3	400	100	4.06	1.02	0.80	6.96	0.10	0.08	3.52	0.02	0.01
4	350	150	3.56	1.53	0.70	7.01	0.15	0.10	3.53	0.03	0.02
5	300	200	3.05	2.04	0.60	7.06	0.20	0.12	3.54	0.03	0.02
6	250	250	2.54	2.54	0.50	7.12	0.26	0.13	3.55	0.04	0.02
7	200	300	2.03	3.05	0.40	7.17	0.31	0.12	3.56	0.05	0.02
8	150	350	1.52	3.56	0.30	7.22	0.36	0.11	3.57	0.06	0.02
9	100	400	1.02	4.07	0.20	7.24	0.38	0.07	3.57	0.07	0.01
10	50	450	0.51	4.58	0.10	7.30	0.44	0.04	3.58	0.07	0.01
11	0	500	0	5.09	0.00	6.86	0.00	0.00	0.00		0.00

9. Distribution diagram for the systems 1^{3+} / $1X^{2+}$ / $1X_2^{+}$ in dmso-d_6 and in D_2O

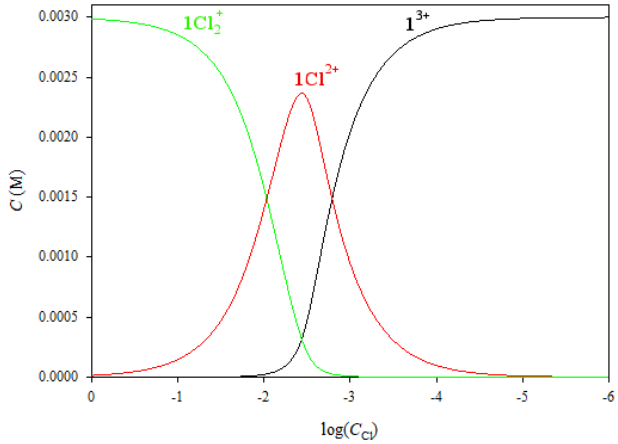

Figure S29: Species distribution diagram as a function of the total chloride concentration in dmso-d_6 ($[\mathbf{1}^{3+}]_0$=0.003M).

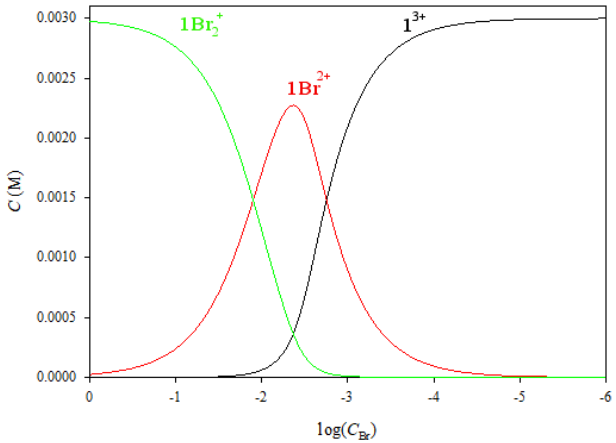

Figure S30: Species distribution diagram as a function of the total bromide concentration in dmso-d_6 ($[\mathbf{1}^{3+}]_0$=0.003M).

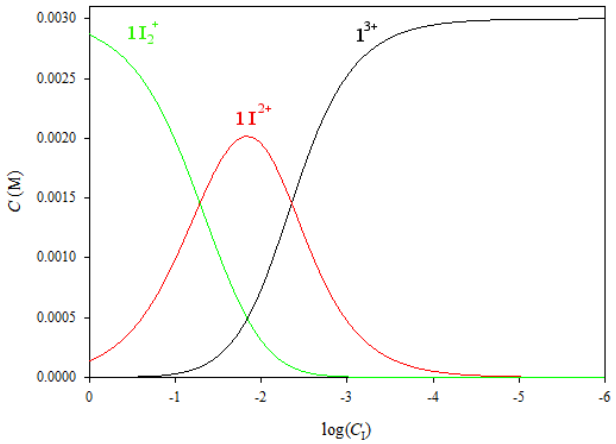

Figure S31: Species distribution diagram as a function of the total iodide concentration in dmso-d_6 ($[\mathbf{1}^{3+}]_0$=0.003M).

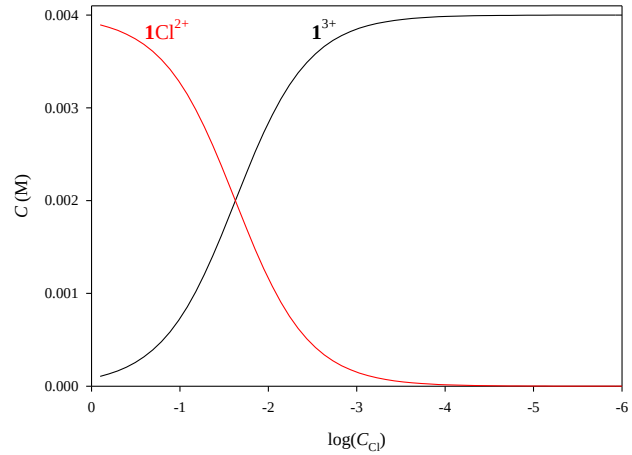

Figure S32: Species distribution diagram as a function of the total chloride concentration in D_2O ($[\mathbf{1}^{3+}]_0$=0.004M).

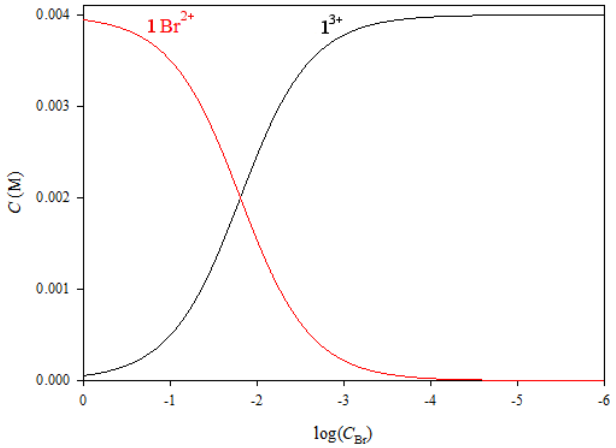

Figure S33: Species distribution diagram as a function of the total bromide concentration in D_2O ($[\mathbf{1}^{3+}]_0$=0.004M).

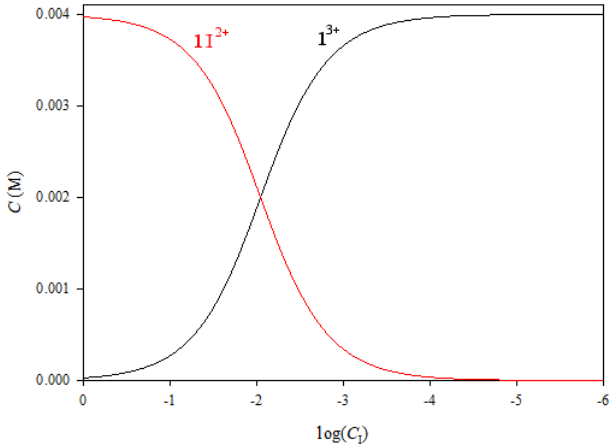

Figure S34: Species distribution diagram as a function of the total iodide concentration in D_2O ($[\mathbf{1}^{3+}]_0$=0.004M).

10. NMR titration of 1-3PF_6 with $NEt_4Cl \cdot H_2O$ in D_2O

Method a

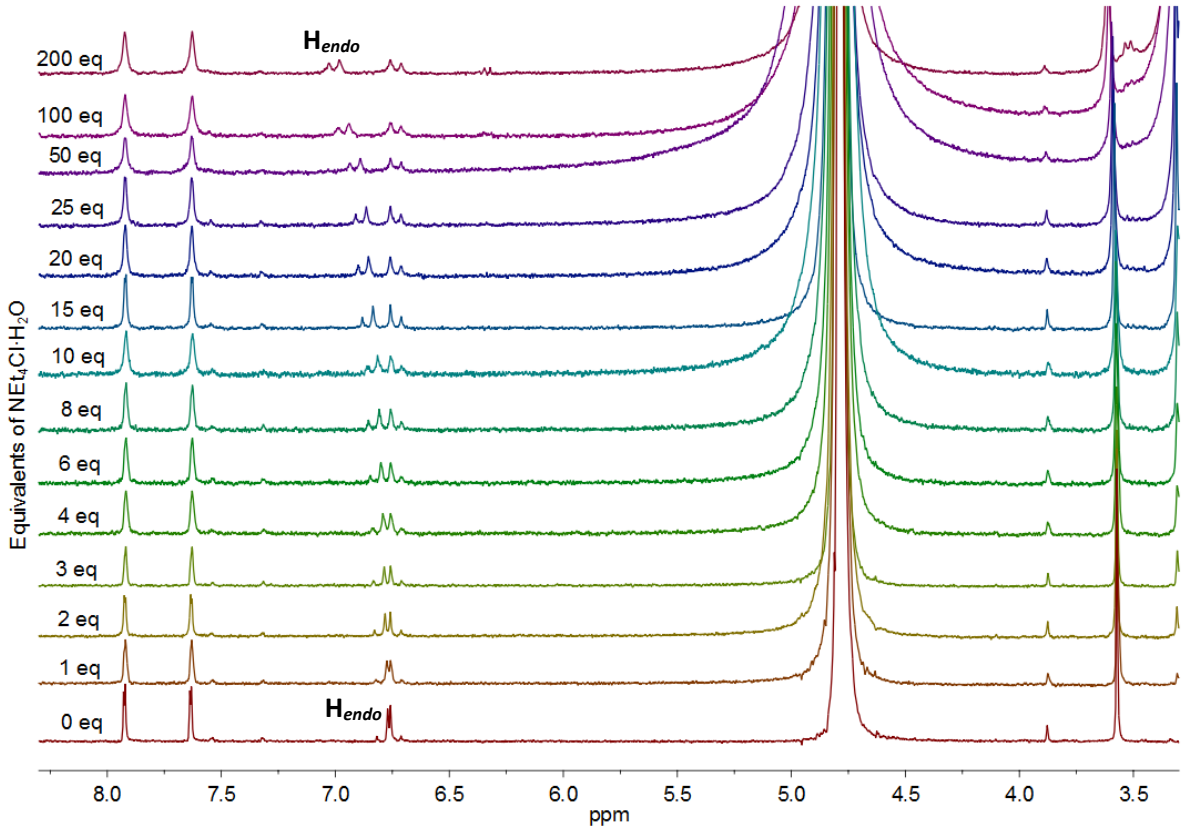

Figure S35: ^{1}H NMR titration (300 MHz, 298 K) of a $4.22 \cdot 10^{-4}$ M solution of **1-3PF_6** in D_2O with a $NEt_4Cl \cdot H_2O$ solution in D_2O.

Table S8: ^{1}H NMR titration (300 MHz, 298 K) of a $4.22 \cdot 10^{-4}$ M solution of **1-3PF_6** in D_2O with a $NEt_4Cl \cdot H_2O$ solution in D_2O.

$[1\text{-}3PF_6]_0$ (mM)	$[Cl^-]_0$ (mM)	$[Cl^-]_0/[1\text{-}3PF_6]_0$	δ H_{endo} (ppm)	Δδ H_{endo} (ppm)
0.422	0.000	0.00	6.7935	0.000
0.420	0.422	1.01	6.7975	0.004
0.418	0.841	2.01	6.8045	0.011
0.416	1.25	3.02	6.809	0.0155
0.414	1.66	4.02	6.813	0.0195
0.410	2.47	6.04	6.8235	0.030
0.406	3.27	8.05	6.832	0.0385
0.402	4.04	10.06	6.8375	0.044
0.393	5.92	15.09	6.8585	0.065
0.384	7.72	20.12	6.8775	0.084
0.375	9.43	25.15	6.887	0.0935
0.338	17.0	50.30	6.9135	0.120
0.338	33.8	100.00	6.9645	0.171
0.338	67.5	200.00	7.005	0.2115

Method b

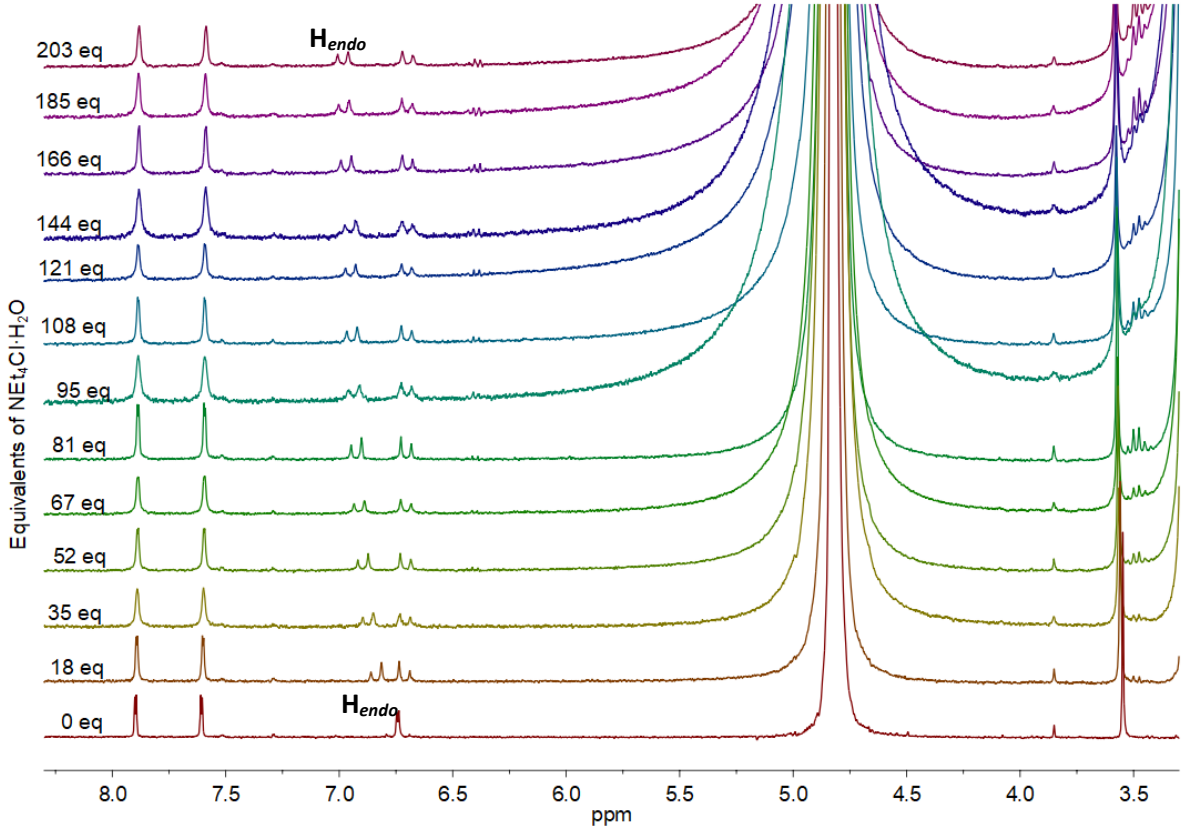

Figure S36: ^{1}H NMR titration (300 MHz, 298 K) of a $4.22 \cdot 10^{-4}$ M solution of **1-3PF$_6$** in D_2O with a $NEt_4Cl \cdot H_2O$ solution in D_2O.

Table S9: ^{1}H NMR titration (300 MHz, 298 K) of a $4.22 \cdot 10^{-4}$ M solution of **1-3PF$_6$** in D_2O with a $NEt_4Cl \cdot H_2O$ solution in D_2O.

$[\mathbf{1\text{-}3PF_6}]_0$ (mM)	$[Cl^-]_0$ (mM)	$[Cl^-]_0/[\mathbf{1\text{-}3PF_6}]_0$	δ H_{endo} (ppm)	$\Delta\delta$ H_{endo} (ppm)
0.422	0.00	0.00	6.7935	0.000
0.422	7.66	18.15	6.86045	0.06695
0.422	14.89	35.29	6.89655	0.10305
0.422	21.74	51.51	6.91865	0.12515
0.422	28.22	66.87	6.9355	0.142
0.422	34.37	81.44	6.9478	0.1543
0.422	40.21	95.29	6.9595	0.166
0.422	45.77	108.46	6.9673	0.1738
0.422	51.06	121.00	6.97405	0.18055
0.422	60.93	144.37	6.9785	0.185
0.422	69.93	165.72	6.99435	0.20085
0.422	78.19	185.28	7.00295	0.20945
0.422	85.78	203.28	7.0084	0.2149

11. NMR titration of 1-3PF$_6$ with NEt$_4$Br in D$_2$O

Method a

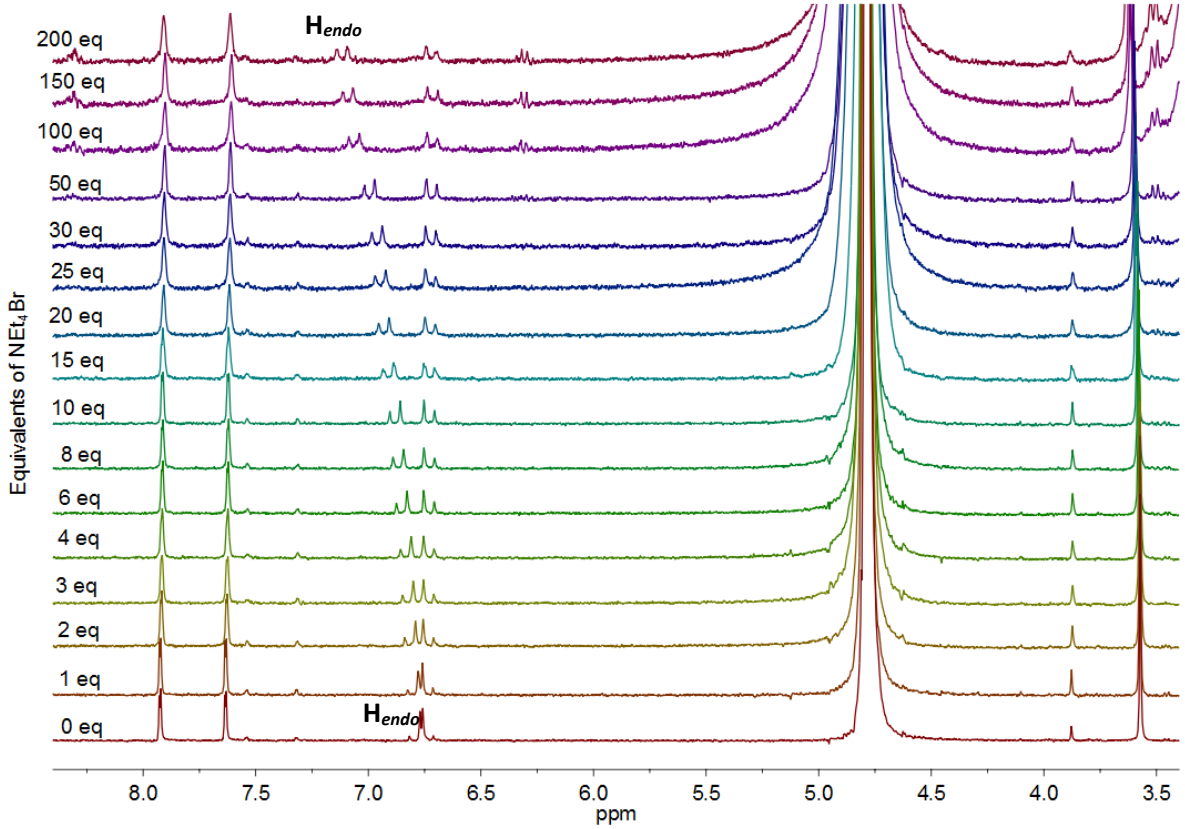

Figure S37: ^{1}H NMR titration (300 MHz, 298 K) of a 4.22·10^{-4} M solution of **1-3PF$_6$** in D$_2$O with a NEt$_4$Br solution in D$_2$O.

Table S10: ^{1}H NMR titration (300 MHz, 298 K) of a 4.22·10^{-4} M solution of **1-3PF$_6$** in D$_2$O with a NEt$_4$Br solution in D$_2$O.

[1-3PF$_6$]$_0$	[Br$^-$]$_0$ (mM)	[Br$^-$]$_0$/[1-3PF$_6$]$_0$	δ H$_{endo}$ (ppm)	Δδ H$_{endo}$ (ppm)
0.422	0.00	0.00	6.7935	0
0.420	0.414	0.99	6.802	0.0085
0.418	0.825	1.97	6.8145	0.021
0.416	1.23	2.96	6.8245	0.031
0.414	1.63	3.95	6.833	0.0395
0.410	2.43	5.92	6.8515	0.058
0.406	3.20	7.90	6.867	0.0735
0.402	3.97	9.87	6.881	0.0875
0.393	5.81	14.80	6.915	0.1215
0.384	7.57	19.74	6.9385	0.145
0.375	9.26	24.67	6.953	0.1595
0.367	10.9	29.61	6.9695	0.176
0.338	16.7	49.35	7.0073	0.2138
0.338	37.5	110.93	7.0802	0.2867
0.338	52.7	156.07	7.1075	0.314
0.338	68.7	203.46	7.128	0.3345

12. NMR titration of 1-3PF$_6$ with NBu$_4$I in D$_2$O

Method a

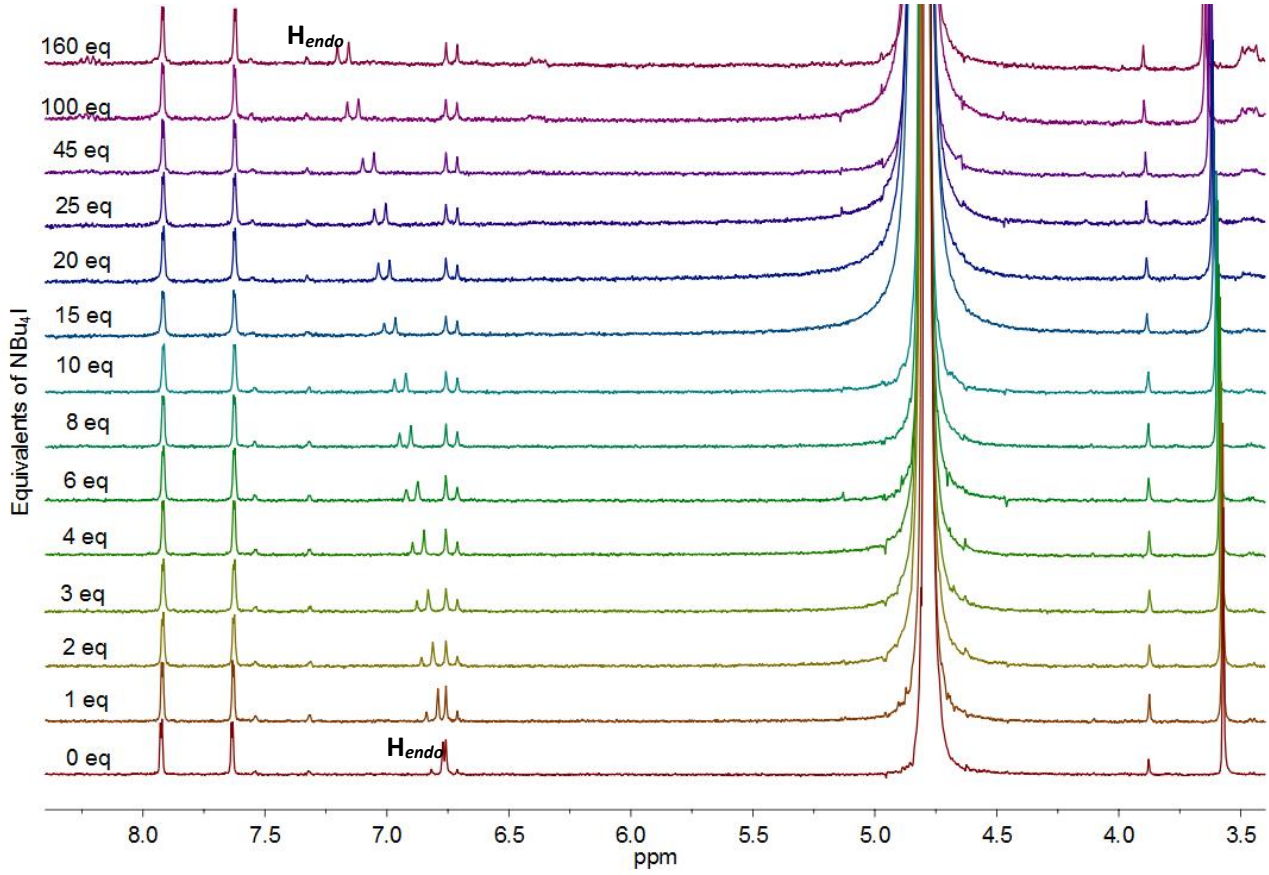

Figure S38: ^{1}H NMR titration (300 MHz, 298 K) of a 4.22·10^{-4} M solution of **1-3PF$_6$** in D$_2$O with a NBu$_4$I solution in D$_2$O.

Table S11: ^{1}H NMR titration (300 MHz, 298 K) of a 4.22·10^{-4} M solution of **1-3PF$_6$** in D$_2$O with a NBu$_4$I solution in D$_2$O.

[1-3PF$_6$]$_0$ (mM)	[I$^-$]$_0$ (mM)	[I$^-$]$_0$/[1-3PF$_6$]$_0$	δ H$_{endo}$ (ppm)	Δδ H$_{endo}$ (ppm)
0.422	0.00	0.00	6.7935	0
0.420	0.414	0.99	6.802	0.0085
0.418	0.825	1.97	6.8145	0.021
0.416	1.23	2.96	6.8245	0.031
0.414	1.63	3.95	6.833	0.0395
0.410	2.43	5.92	6.8515	0.058
0.406	3.20	7.90	6.867	0.0735
0.402	3.97	9.87	6.881	0.0875
0.393	5.81	14.80	6.915	0.1215
0.384	7.57	19.74	6.9385	0.145
0.375	9.26	24.67	6.953	0.1595
0.367	10.9	29.61	6.9695	0.176
0.338	16.7	49.35	7.0073	0.2138
0.338	37.5	110.93	7.0802	0.2867
0.338	52.7	156.07	7.1075	0.314
0.338·	68.7	203.46	7.128	0.3345

13. NMR titration of 1-3PF_6 with HCl in D_2O

Method a

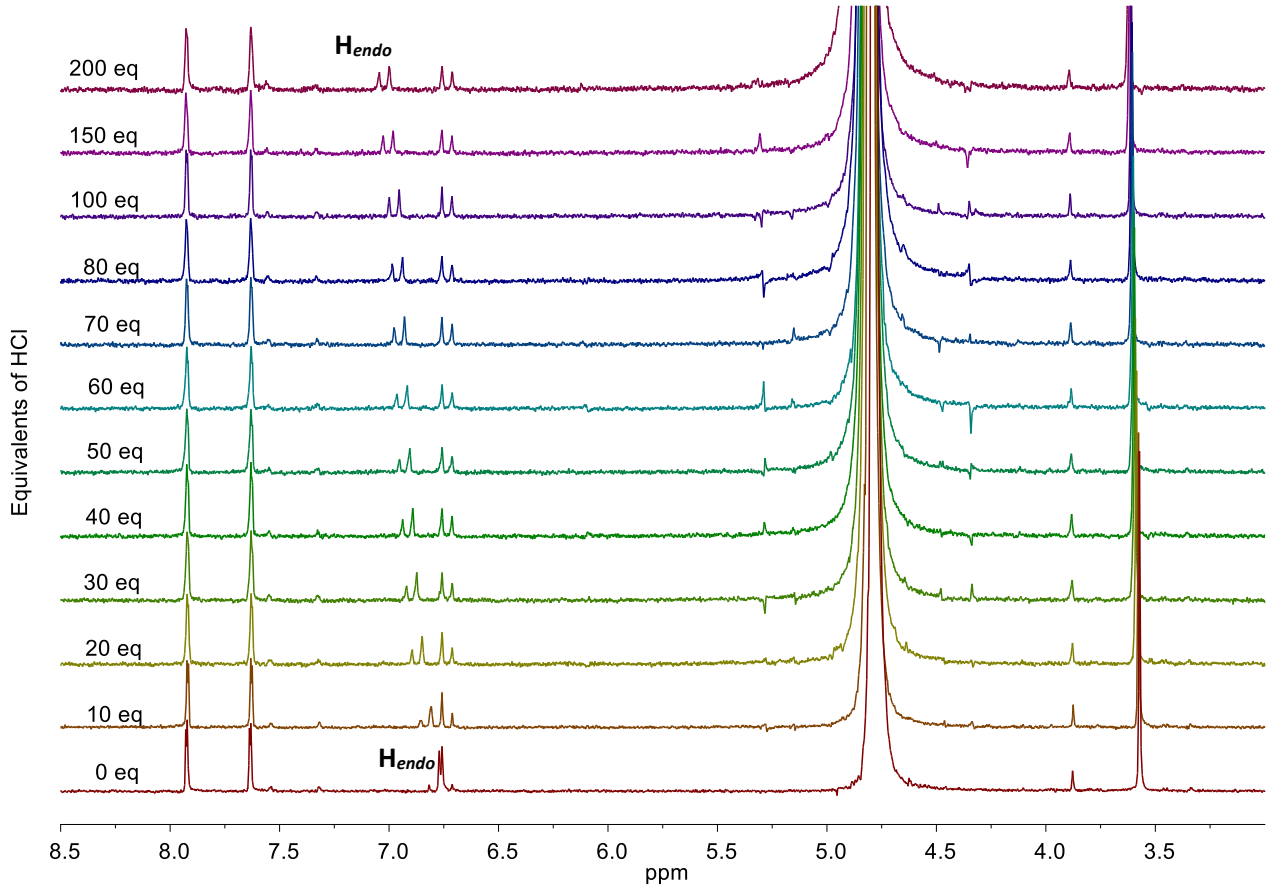

Figure S39: ^{1}H NMR titration (300 MHz, 298 K) of a $4.22 \cdot 10^{-4}$ M solution of **1-3PF_6** in D_2O with a HCl solution in D_2O.

Table S12: ^{1}H NMR titration (300 MHz, 298 K) of a $4.22 \cdot 10^{-4}$ M solution of **1-3PF_6** in D_2O with a HCl solution in D_2O.

$[1\text{-}3PF_6]_0$ (mM)	$[Cl^-]_0$ (mM)	pH	$[Cl^-]_0/[1\text{-}3PF_6]_0$	δ H_{endo} (ppm)	Δδ H_{endo} (ppm)
0.422	0.00	7.00	0	6.795	0
0.418	4.178	2.38	10	6.835	0.04
0.414	8.271	2.08	20	6.87	0.075
0.410	12.29	1.91	30	6.895	0.1
0.406	16.24	1.79	40	6.915	0.12
0.402	20.09	1.70	50	6.93	0.135
0.398	23.88	1.62	60	6.94	0.145
0.395	27.62	1.56	70	6.955	0.16
0.391	31.26	1.50	80	6.96	0.165
0.384	38.36	1.42	100	6.975	0.18
0.367	55.07	1.26	150	7.005	0.21
0.352	70.31	1.15	200	7.02	0.225

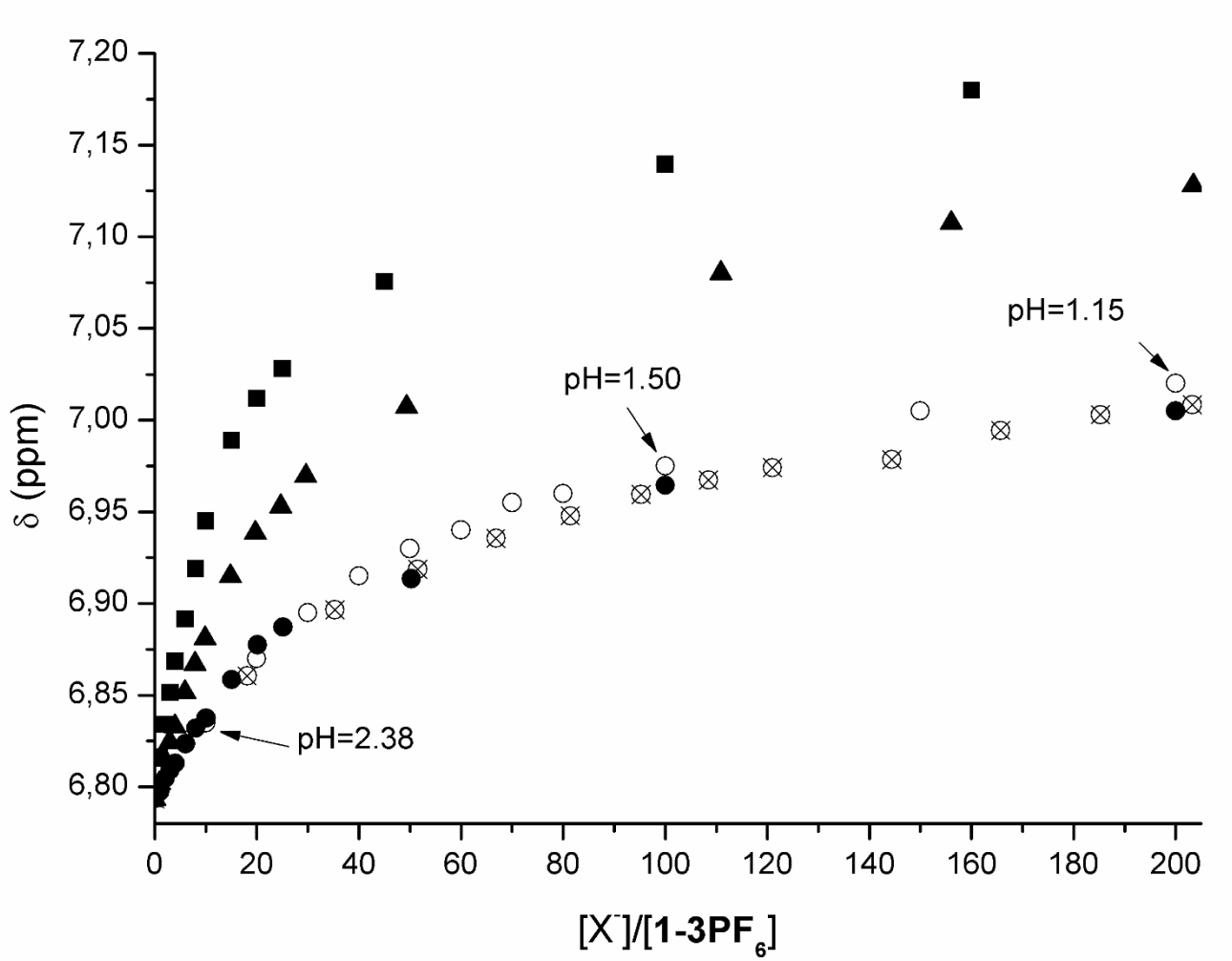

Figure S40: ^{1}H NMR titration curves (300 MHz, 298 K) based on the H_{endo} chemical shift variation of a $4.22 \cdot 10^{-4}$ M solution of **1-3PF$_6$** in D_2O with a HCl (○), $NEt_4Cl \cdot H_2O$ (●, method a), $NEt_4Cl \cdot H_2O$ (⊗, method b), NEt_4Br (▲) and NBu_4I (■) solution in D_2O.

14. NMR titration of 1-3PF_6 with NBu_4PF_6 in DMSO-d_6

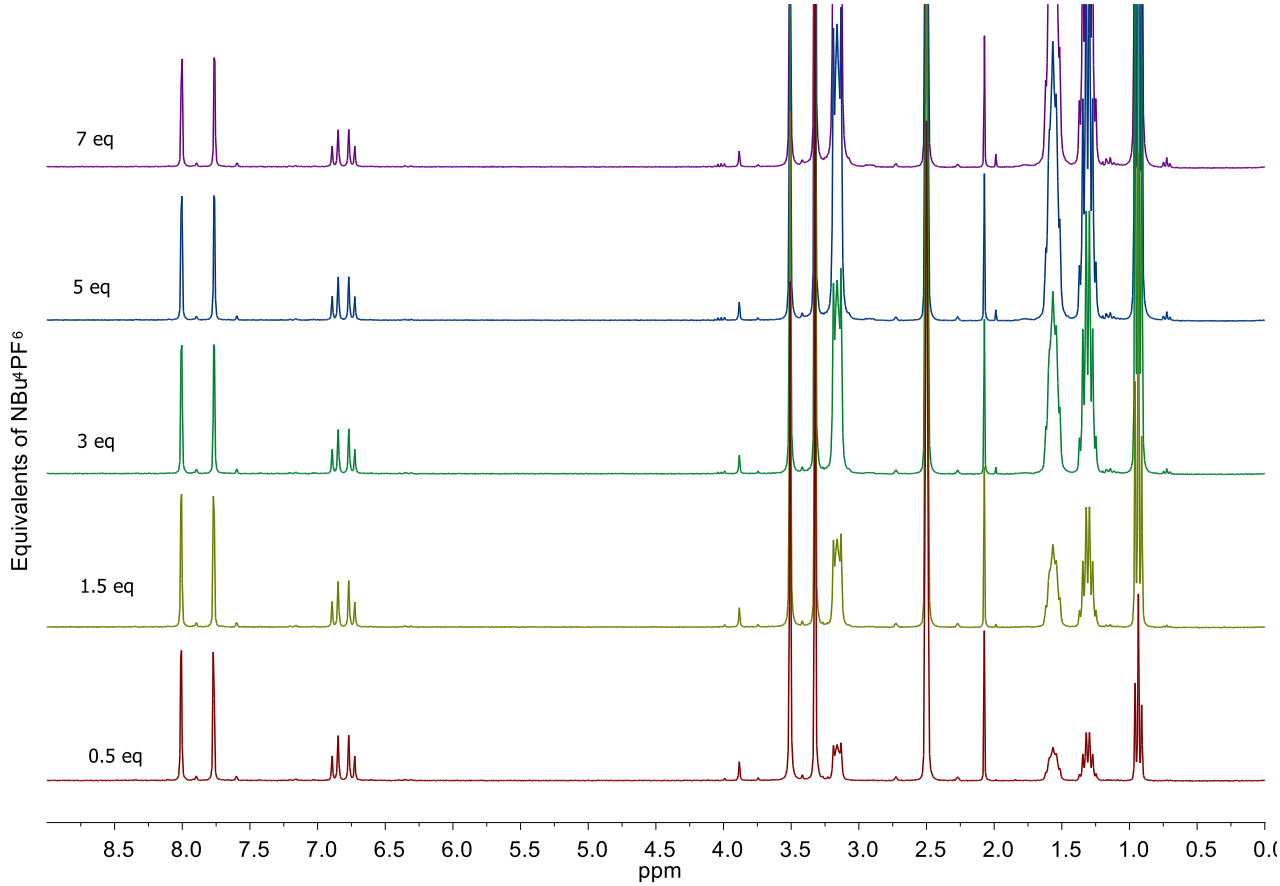

Figure S41: ^{1}H NMR titration (300 MHz, 298 K) of a $7.26 \cdot 10^{-3}$ M solution of **1-3PF_6** in DMSO-d_6 with a NBu_4PF_6 solution in DMSO-d_6.

15. Additional computational data

Table S13: Percentage composition (halogen p orbitals and $\mathbf{1}^{3+}$ LUMO) of frontier MOs of $\mathbf{1X}^{2+}$ complexes from ASM; level of theory: ZORA-BLYP-D3(BJ)/TZ2P sc.

	HOMO-2 (A')	HOMO-1 (A'')	HOMO (A')	LUMO (A'')
$\mathbf{1Cl}^{2+}$	41.33% Cl(p_x) 39.77% Cl(p_y) 7.69% AuL^{3+}(LUMO)	90.03% Cl(p_z) 3.72%AuL^{3+}(LUMO)	49.98% Cl(p_x) 34.16% Cl(p_y) 3.72% AuL^{3+}(LUMO)	99.7% AuL^{3+}(LUMO+1)
$\mathbf{1Br}^{2+}$	20.17% Cl(p_x) 56.37% Cl(p_y) 12.31% AuL^{3+}(LUMO)	91.19% Br(p_z) 1.14%AuL^{3+}(LUMO)	71.97% Br (px) 17.60% Br (py) 1.55% AuL^{3+}(LUMO)	99.7% AuL^{3+}(LUMO+1)
$\mathbf{1I}^{2+}$	15.10% I(p_x) 60.27% I(p_y) 16.23% AuL^{3+}(LUMO)	92.48% I(p_z)	76.82% I(p_x) 13.96% I(p_y) 1.07% AuL^{3+}(LUMO)	99.75% AuL^{3+}(LUMO+1)

Table S14: Energies (kcal mol^{-1}) of the reactions of formation of $AuLX^{2+}$ and $AuLX_2^+$ (X=Cl, Br, I) in gas-phase, DMSO and water; values in italics refer to energies of species relaxed in solvent. Level of theory (COSMO)-ZORA--BLYP-D3(BJ)/TZ2P sc.

	$\mathbf{1Cl}^{2+}$	$\mathbf{1Br}^{2+}$	$\mathbf{1I}^{2+}$	$\mathbf{1Cl_2}^{+}$	$\mathbf{1Br_2}^{+}$	$\mathbf{1I_2}^{+}$
GAS-PHASE	-235.23	-229.08	-224.08	-397.37	-385.89	-375.51
DMSO	-3.83	-4.92	-6.49	-4.89	-7.04	-10.03
	-5.28	*-5.94*	*-7.00*	*-7.18*	*-8.89*	*-11.09*
H_2O	0.65	-0.53	-2.17	2.05	-0.59	-3.59
	-1.66	*-2.37*	*-3.32*	*-1.75*	*-3.43*	*-5.41*

16. SC-XRD Data

Table S15: Main crystallographic parameters of compounds **1-Cl,2I$_3$, 1-3Br·I$_2$** and **1-3I$_3$**.

Compound	**1-Cl,2I$_3$**	**1-3Br·I$_2$**	**1-3I$_3$**
Formula	C_{18} H_{24} Au N_8 Cl I_6	C_{18} H_{24} Au N_8 Br_3 I_2	C_{22} H_{30} Au I_9 N_{10}
Molecular Weight	1346.27	1042.95	1773.62
Crystal system	monoclinic	monoclinic	orthorhombic
Space group	C 2/c	C 2/m	P b c a
a[Å]	13.237(6)	12.0405(8)	21.3052(16)
b[Å]	21.466(10)	11.2536(8)	14.9146(11)
c[Å]	12.233(6)	10.3517(7)	27.057(2)
β[°]	108.518(7)	104.686(7)	90
V[Å^3]	3296(3)	1356.82(17)	8597.5(11)
Z	4	2	8
D_{calc}[g·cm^{-3}]	2.713	2.553	2.740
μ[cm^{-1}]	10.186	12.137	9.913
F(000)	2408	956	6304
θ_{max} [°]	30.436	28.994	29.481
Reflections collected	22910	9679	126682
Independent reflections	4870	1983	11903
Reflections in refinement	3518	1976	6582
R(int)	0.0777	0.0298	0.0439
Refined parameters	160	82	385
R_1 [I > 2σ(I)]	R_1 = 0.0768 wR_2 = 0.1906	R_1 = 0.0321 wR_2 = 0.0872	R_1 = 0.0501 wR_2 = 0.1285
wR_2 [all data]	R_1 = 0.0964 wR_2 = 0.2072	R_1 = 0.0321 wR_2 = 0.0873	R_1 = 0.1031 wR_2 = 0.1555
GOF	0.958	0.999	1.058

$R_1 = \Sigma|Fo-Fc|/\Sigma(Fo)$; $wR_2 = [\Sigma[w(Fo^2-Fc^2)^2]/\Sigma[w(Fo^2)^2]]^{1/2}$.

17. Additional comments on crystal packing

1-Cl,2I$_3$

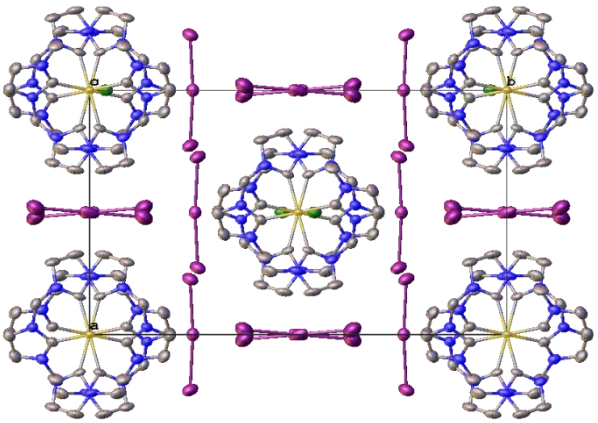

View of the crystal packing of **1-Cl,2I$_3$** along the *c* axis.

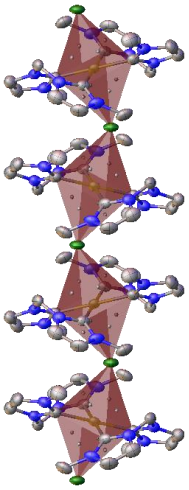

View along the *a* axis of the –[Au-Cl]$_n$- lines.

In the crystal packing of **1-Cl,2I$_3$** the cationic gold(III) complexes are stacked together, with a chloride in between each pseudo-planar cationic complex. Every chloride is interacting with two different gold centres with an Au-Cl distance of 3.1691(17) Å, forming –[Au-Cl]$_n$- lines, running in the *c* crystallographic direction. Two tricationic complexes interacting with the same chloride are rotated one each other, with a torsion angle C1-Au-Au'-C9' of 116.7(4)° (' = -x, +y, 5/2-z). The I_3^- anions lays in the crystal packing in between the -[Au-Cl]$_n$- lines. There are no interactions between the I_3^- anions and the gold centres, although there are different short contacts between the terminal atoms of the I_3^- groups and hydrogen atoms of the diNHC ligands. The I-I distances in the I_3^- groups are fully consistent with those of the I_3^- groups present in the structure of **1-3I$_3$** that are not involved in the Au-I interaction (*vide infra*).

1-3Br·I_2

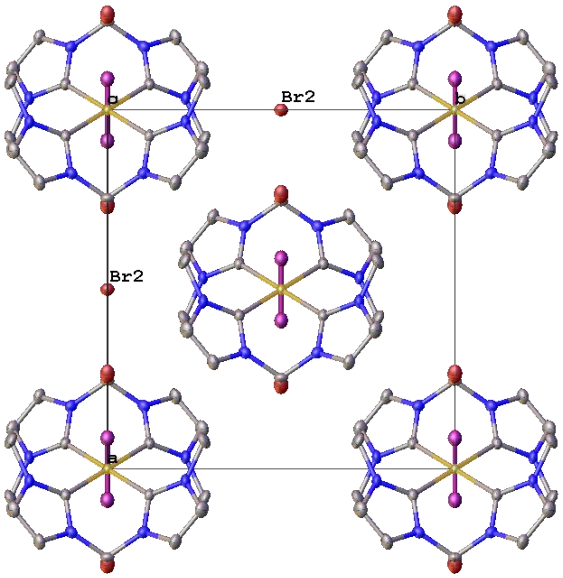

View of the crystal packing of **1-3Br·I_2** along the *c* axis.

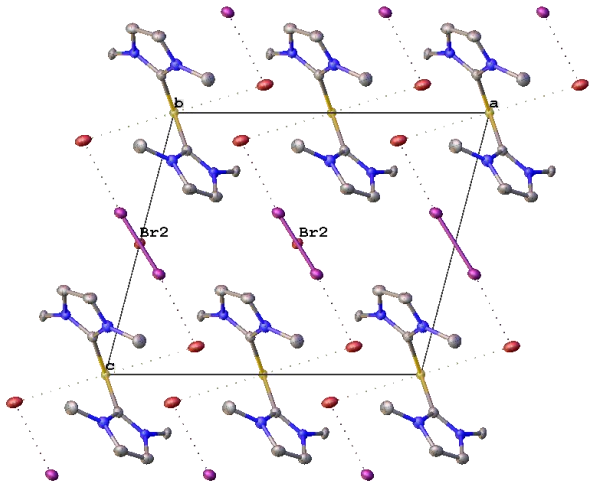

View of the crystal packing of **1-3Br·I_2** along the *b* axis.

The crystal packing of **1-3Br·I_2**, is formed by **1-Br^{2+}** lines, running along the *c* crystallographic direction. In this case the bromides interacting with the gold centres are not in a bridging fashion in between two gold centres, thus discrete units of **1-Br_2^+** are found in the lattice. An I_2 molecule is found in between two next gold centres laying on the same axis. This I_2 molecule, presents short contacts with two bromides interacting with the gold centres. In this way, a zigzag -$[AuBrI_2Br]_n$- chain running along the *c* crystallographic direction is formed. The Br1-I1 distance is of 3.1188(6) Å, while the I1-I1' distance is of 2.7600(6) Å. The Br2 atoms are not interacting with the gold centres but they present short contacts towards hydrogen atoms of the diNHC ligands, and they are located in between the **1-Br_2^+** lines.

1-3I$_3$

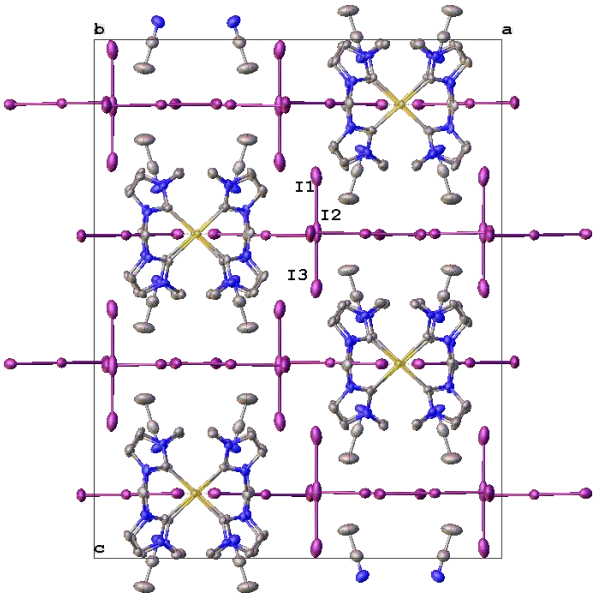

View of the crystal packing of **1-3I$_3$** along the *b* axis.

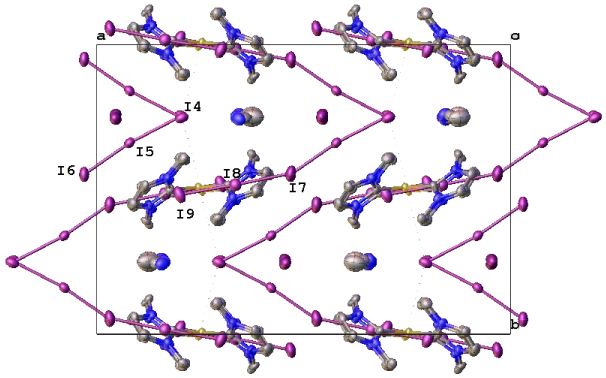

View of the crystal packing of **1-3I$_3$** along the *c* axis.

In the packing of **1-3I$_3$**, lines of gold complexes are ordered along the b crystallographic axes. Two next complexes on the same line, interact with the same iodine atom of an I_3^- group, which is therefore in a bridging fashion, forming -[Au-I]$_n$- lines along the b axes. The iodine atom involved in the Au-I interaction is only I4, with the Au-I4' and Au-I4'' distances of 3.6834(7) and 4.0182(7) Å respectively (' = 2-x, -1/2+y, 3/2-z, '' = -1/2+x, +y, 3/2-z). As a consequence of the interaction between I4 and the gold centres, the I4-I5 distance is longer (3.0251(10)Å) compared to the other I-I distances present in the structure (I1-I2 2.9136(19), I2-I3 2.9324(19), I5-I6 2.8418(10), I7-I8 2.9027(11), and I8-I9 2.9274(11) Å). The I_3^- anions that are not involved in the Au-I interaction lays in between the -[AuI]$_n$-lines. The acetonitrile molecules present in crystal lattice, are in the space between the gold complexes in the different lines. Several hydrogen bond interactions between the I_3^- anions and the hydrogen atoms of the diNHC ligands and of the acetonitrile molecules are present.